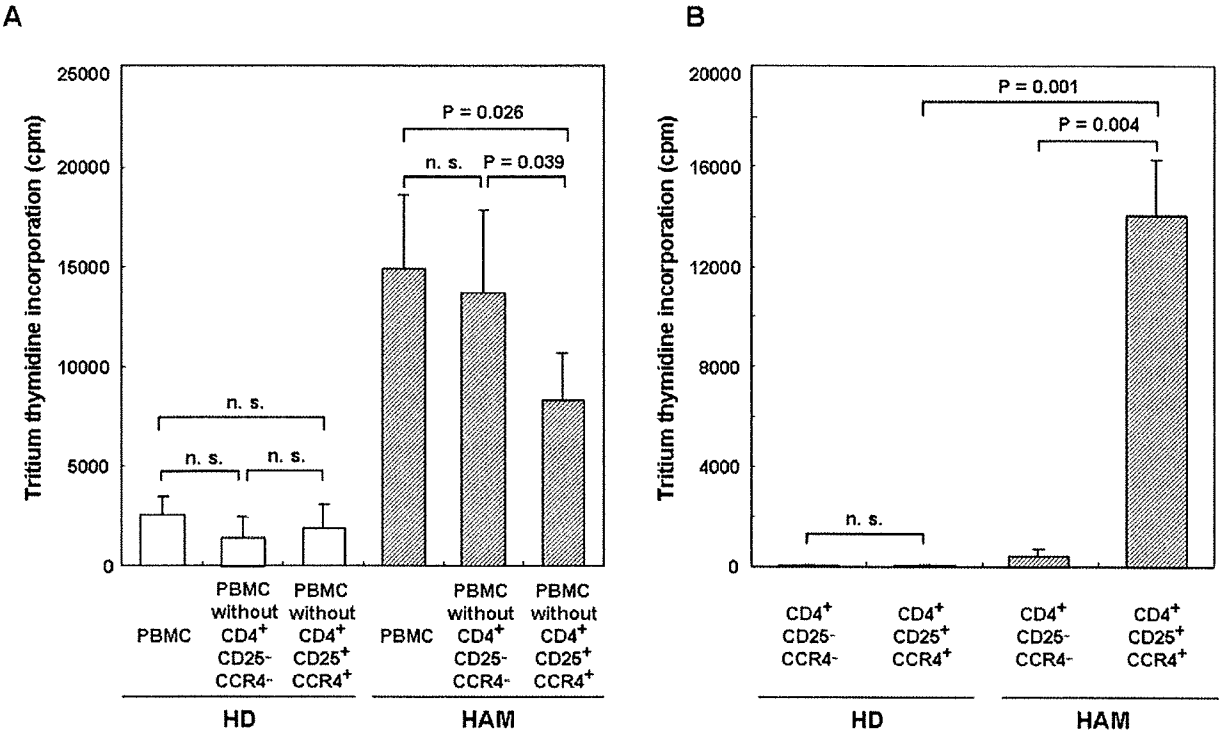

Figure 8. Removal of CD4+CD25+CCR4+ T cells decreases spontaneous proliferation of PBMCs from HAM/TSP patients. A. PBMCs, PBMC lacking $CD4^+CD25^+CCR4^+$, and PBMCs lacking $CD4^+CD25^-CCR4^-$ obtained using FACS sorting from 4 HDs and 4 HAM/TSP patients were cultured for 7 days, and the magnitude of proliferation was compared. Data are presented as mean±SE. The P values are calculated by paired *t* test. n.s. not significant. **B.** $CD4^+CD25^+CCR4^+$ T cells of HAM/TSP patients proliferated independently. $CD4^+CD25^+CCR4^+$ cells and $CD4^+CD25^-CCR4^-$ T cells were separated by FACS sorting from 4 HDs and 4 HAM/TSP patients, cultured for 7 days, and the magnitude of proliferation was compared. Data are presented as mean±SE. The P values within each group are calculated by paired *t* test and those between the HD and HAM groups, by unpaired Student's *t* test. n.s. not significant.
doi:10.1371/journal.pone.0006517.g008

we and other researchers have demonstrated that $CD4^+CD25^+$ T cells exhibit reduced Foxp3 expression and Treg suppression [20,27–29]. Furthermore, it has been demonstrated that HTLV-1-infected $CD4^+$ T cells in HAM/TSP patients produce Th1 cytokines (IFN-γ) [20,32]. Therefore, it was expected that $CD4^+CD25^+$ T cells might exhibit reduced CCR4 expression in HAM/TSP patients. However, we clearly demonstrated that CCR4 was selectively overexpressed on HTLV-1-infected T cells. We also demonstrated that the majority of $CD4^+CD25^+CCR4^+$ T cells were infected with HTLV-1 and that this T cell subset was increased in HAM/TSP patients (Figure 1). Furthermore, $CD4^+CD25^+CCR4^+$ T cells, which mainly include suppressive T cell subsets such as Th2 and Treg in HTLV-1-seronegative healthy controls [26], become Th1-like cells with overproduction of IFN-γ and production of low levels of IL-4 and IL-10 (Figures 4 and 5) in patients with HAM/TSP. It is noteworthy that this functional alteration in cytokine production was specific to the HTLV-1-infected $CD4^+CD25^+CCR4^+$ T cell subtype (Figure 5B). These results suggest that HTLV-1-infected $CD4^+CD25^+CCR4^+$ T cells in HAM/TSP patients were functionally proinflammatory rather than suppressive. A hallmark of hyperimmune responsiveness in HAM/TSP is the capacity of PBMCs to spontaneously proliferate, and the removal of $CD4^+CD25^+CCR4^+$ T cells diminished this proliferative response (Figure 8A). Recently, Shimizu et al reported that the depletion of $CCR4^+$ cells reduced IFN-γ production in the supernatant of cultured antigen-responding cells in HAM/TSP patients [44]. Thus, functionally altered $CD4^+CD25^+CCR4^+$ T cells in HAM/TSP patients are a necessary component of the accelerated lymphoproliferative response.

Patients with HAM/TSP exhibit a chronic inflammatory disorder characterized by accumulation of activated $CD4^+$ and $CD8^+$ T cells [38]. $CD4^+CD25^+$ T cells from HAM/TSP patients also exhibit an activated phenotype marked by decreased expression of CD45RA together with increased expression of IFN-γ compared to the same subset in healthy individuals [20]. Furthermore, we previously demonstrated that HTLV-1 *tax* overexpression was capable of reducing Foxp3 expression, and the HTLV-1 *tax* mRNA expression in PBMCs of HAM/TSP was elevated [8,20]. Therefore, we hypothesized that persistent T cell activation in patients with HAM/TSP triggered by viral antigens such as HTLV-1 *tax* together with the downregulation of Foxp3 may result in decline of the $CD4^+CD25^+CCR4^+Foxp3^+$ Treg population and accumulation of Foxp3-negative $CD4^+CD25^+CCR4^+$ T cells that lack suppressive function, but are capable of exacerbating the disease process. In this study, we have demonstrated that $CD4^+CD25^+CCR4^+Foxp3^-$ T cells were proliferating *in vivo* (Ki67 positive) (Figure 3), and the frequency of this population was increased in HAM/TSP patients (Figure 2). Moreover, analysis of the cytokine expression in this $CD4^+CD25^+CCR4^+Foxp3^-$ T cell subset demonstrated that these cells were unique because they produce multiple proinflammatory cytokines such as IL-2, IL-17, and few IFN-γ in healthy individuals while $CD4^+CD25^+CCR4^+Foxp3^+$ T cells (Treg cells) did not (Figure 4). Furthermore, it was demonstrated that HAM/TSP patients exhibited

only few $CD4^+CD25^+CCR4^+Foxp3^+$ T cells that do not produce such cytokines (Figure 3). Rather, the $CD4^+CD25^+CCR4^+Foxp3^-$ T cells in HAM/TSP were increased and found to overproduce IFN-γ (Figures 3 and 4). Further, the frequency of these IFN-γ-producing $CD4^+CD25^+CCR4^+Foxp3^-$ T cells may have a functional consequence since this population was associated with increased clinical disease activity and severity in HAM/TSP (Figure 7). These results suggest that IFN-γ-producing $CD4^+CD25^+CCR4^+Foxp3^-$ T cells may play an important pathogenic role in HAM/TSP by augmenting inflammation in the CNS. Thus, we have defined a unique T cell subset—IFN-$\gamma^+CCR4^+Foxp3^-CD4^+CD25^+$ T cells—that is specifically increased in HAM/TSP (tentatively designated T_{HAM} cells) and is rarely encountered in healthy individuals. Since some HAM/TSP patients are known to experience complications with other autoimmune disorders [5,6], it would be of interest to determine if this newly defined T cell subset (T_{HAM} cells: IFN-$\gamma^+CCR4^+Foxp3^-CD4^+CD25^+$ T cells) may also be abnormally increased and functionally deregulated in other immunological diseases.

Although $CD4^+CD25^+CCR4^+$ T cells are predominantly infected by HTLV-1 in both HAM/TSP and ATL (Figure 6), it was demonstrated that the ratio of T_{HAM} cells ($CCR4^+Foxp3^-$ with IFN-γ production) to Treg cells ($CCR4^+Foxp3^+$ with no cytokine production) in the $CD4^+CD25^+CCR4^+$ T cell subset were high in HAM/TSP and low in ATL (Figure 2). This differential T_{HAM}/Treg ratio in HTLV-1-infected T cells may be associated with the different immune responses observed between HAM/TSP and ATL. ATL patients have very low frequencies of Tax-specific $CD8^+$ T cells in PBMCs and tend to develop opportunistic infections [21], while HAM/TSP is characterized by extraordinarily high levels of Tax-specific $CD8^+$ CTL [7,8,11,40,41]. It has been reported that the immunosuppressive function of $CD4^+CD25^+$ T cells with high expression of Foxp3 in ATL patients is intact [42]. Thus, the $CD4^+CD25^+CCR4^+$ leukemia T cells with increased Treg function may also contribute to the clinically observed cellular immunodeficiency in ATL patients. However, HAM/TSP patients show extremely high cellular and humoral immune responses such as high frequencies of Tax-specific $CD8^+$ T cells as well as cytomegalovirus (CMV)-specific $CD8^+$ T cells in PBMCs [7,8,28]; high antibody titer to HTLV-1 [6]; and increased production of proinflammatory cytokines such as IL-6, IL-12, and IFN-γ [9]. It has been reported that HAM $CD4^+CD25^+$ T cells with low expression of Foxp3 [20] or HTLV-1 Tax-expressing $Foxp3^+$ Treg cells [45] are defective in their immunosuppressive function. Here, we demonstrate that HTLV-1-infected IFN-γ overproducing $CD4^+CD25^+CCR4^+Foxp3^-$ T cells (T_{HAM} cells) are increased in HAM/TSP patients, and these levels can be correlated with disease severity. Thus, $CD4^+CD25^+CCR4^+$ T cells with increased proinflammatory function together with a defective Treg compartment [20,27–29] may overcome the regulatory effect of HTLV-1-uninfected Treg cells [45] and at least partly account for the heightened immune response observed in HAM/TSP patients. Collectively, these observations support the hypothesis that imbalance of the T_{HAM}/Treg ratio in HTLV-1-infected $CD4^+CD25^+CCR4^+$ T cells is an important factor that contributes to immunological differences of the host immune response between HAM/TSP and ATL (Figure S2).

The high Foxp3 expression without cytokine production and low Foxp3 expression with cytokine production in $CD4^+CD25^+CCR4^+$ T cells (Figure 3A) are consistent with recent reports demonstrating that Foxp3 can target and repress the transcriptional activity of NFAT-AP-1 complexes present at the cytokine promoter [43]. We have previously reported that overexpression of HTLV-1 *tax* was capable of reducing Foxp3 expression [20]. As we have demonstrated high HTLV-1 *tax* expression in HAM/TSP $CD4^+CD25^+CCR4^+$ T cells ($Foxp3^-$) and low HTLV-1 *tax* expression in ATL $CD4^+CD25^+CCR4^+$ T cells ($Foxp3^+$) (Figure 6), it was suggested that HTLV-1 expression intracellularly may act as a "switch" that directs T cell differentiation of $CD4^+CD25^+CCR4^+$ T cells from $Foxp3^+$ to IFN-γ^+Foxp3^- T cells. Further, the increased IFN-γ production and decreased IL-17 production in $CD4^+CD25^+CCR4^+Foxp3^-$ T cells of HAM/TSP patients (Figures 4 and 5) suggests that HTLV-1 expression may also contribute to the differentiation of Th1 versus Th17 $CD4^+$ T cells. These hypotheses are currently under investigation to elucidate the precise molecular mechanisms by which HTLV-1 influences the fate and function of $CD4^+CD25^+CCR4^+$ T cells.

In conclusion, we have defined a unique T cell population (T_{HAM} cells: IFN-$\gamma^+CCR4^+Foxp3^-CD4^+CD25^+$ T cells) that are rarely encountered in normal individuals, are infected by HTLV-1, and are found to be abnormally increased and proinflammatory and correlate with disease severity in HAM/TSP patients. This study is the first to demonstrate that T_{HAM} cells are crucial for the pathogenesis of this retrovirus-associated chronic inflammatory disorder of the nervous system.

Materials and Methods

Subjects, cell preparation, and determination of CSF neopterin concentrations

A total of 11 HAM/TSP patients, 8 healthy donors, and 5 ATL patients (chronic type) participated in this study. Written informed consents were obtained from all the subjects in accordance with the Declaration of Helsinki as part of a clinical protocol reviewed and approved by the Institutional Ethics Committee (St. Marianna University). Blood samples were collected from the subjects, peripheral blood mononuclear cells (PBMCs) were separated by centrifugation over Ficoll-Hypaque gradients, and the cells were cryopreserved in liquid nitrogen until testing. HAM/TSP was diagnosed according to the guidelines defined by the WHO, and ATL was diagnosed on the basis of the criteria proposed by Shimoyama [46]. HTLV-1 seropositivity was determined by particle agglutination (Serodia-HTLV-1; Fujirebio, Japan) and confirmed by western blotting (SRL, Japan). Clinical disease severity was evaluated by Osame's motor disability scale (Table 1) [6]. In some experiments, $CD4^+$ T cells were negatively selected from the PBMCs by using magnetic beads (MACS $CD4^+$ T cell isolation kit; Miltenyi Biotec, Germany), according to the manufacturer's instructions. FACS cell sorting was performed using JSAN (Bay Bioscience, Japan), and purity after sorting was approximately 99% (Figure S1). Neopterin concentration was measured by high-performance liquid chromatography with fluorometric detection methods [33] (SRL, Japan).

Flow cytometry

Cells were immunostained with various combinations of the following fluorescence-conjugated antibodies that served as cell surface markers: CD4 (OKT4; eBioscience, San Diego, CA), CD25 (M-A251; BD Biosciences, San Diego, CA), CCR4 (1G1; BD Biosciences). In some experiments, cells were fixed by a staining buffer set (eBioscience), then intracellularly stained with the antibodies to Foxp3 (PCH101; eBioscience) and Ki67 (B56; BD Biosciences). For intracellular cytokine staining, the cells were stimulated for 5 h with phorbol 12-myristate 13-acetate (PMA) and ionomycin (Sigma, Japan) in the presence of monensin (Golgistop; BD Biosciences). Cells were fixed and stained with the antibodies to IFN-γ (B27; BD Biosciences), IL-2 (MQ1-17H12; BD Biosciences), IL-10 (JES3-9D7, eBioscience), and IL-17A (eBio64-

Table 1. Motor disability grading for HAM/TSP.

Grade	Motor disability
0	Normal gait and running
1	Normal gait but runs slowly
2	Abnormal gait (staggering or spastic)
3	Abnormal gait and unable to run
4	Needs support while using stairs but walks without assistance
5	Needs one hand support in walking
6	Needs two hands support in walking (can walk more than 10 meter)
7	Needs two hands support in walking (can walk less than 10 meter)
8	Needs two hands support in walking (can walk less than 5 meter)
9	Unable to walk but can walk on all fours
10	Unable to walk on all fours but can crawl with hands
11	Unable to crawl with hands but can turn sideways in bed
12	Unable to turn sideways but can move the toes
13	Completely bedridden (unable to move the toes)

doi:10.1371/journal.pone.0006517.t001

DEC17; eBioscience). Flow cytometric analysis was performed on a FACSCalibur cytometer (BD Biosciences). Data processing was performed using FlowJo software (TreeStar, San Diego, CA).

Real-time PCR

The HTLV-1 proviral DNA load was measured as previously described [8]. For the real-time reverse transcriptase-PCR (RT-PCR) analysis, $CD4^+CD25^+CCR4^+$ cells were separated by FACS sorting from 3 HDs, 4 HAM/TSP patients, and 3 ATL patients. The number of subjects for RT-PCR was limited because a large number of PBMCs are required for sorting a sufficient number of $CD4^+CD25^+CCR4^+$ cells for the analysis. Total RNA was isolated from cells using ISOGENE (Nippon Gene, Japan). The first-strand cDNA was synthesized with random hexamers and reverse transcriptase (ReverTraAce; Toyobo, Japan) using 1 μg of total RNA in a reaction volume of 20 μl. Real-time PCR reactions were carried out using TaqMan Universal Master Mix (Applied Biosystems) and Universal Probe Library assays designed using ProbeFinder software (Roche Applied Science). The primer sequences and Universal Probe numbers used are available upon request (Roche Applied Science). ABI Prism 7500 SDS was programmed to an initial step of 2 min at 50°C and 10 min at 95°C, followed by 45 cycles of 15 sec at 95°C and 1 min at 60°C. The primers used were as follows: IFN-γ, 5′-GGCATTTTGAAGAATTGGAAAG-3′ (forward) and 5′-TTTGGATGCTCTGGTCATCTT-3′ (reverse) (probe No. 21); IL-2, 5′-AAGTTTTACATGCCCAAGAAGG-3′ (forward) and 5′-AAGTGAAAGTTTTTGCTTTGAGCTA-3′ (reverse) (probe no. 65); IL-17A, 5′-TGGGAAGACCTCATTGGTGT-3′ (forward) and 5′-GGATTTTCGTGGGATTGTGAT-3′ (reverse) (probe No. 8); and GAPDH, 5′-AGCCACATCGCTCAGACA-3′ (forward) and 5′-GCCCAATACGACCAAATCC-3′ (reverse) (probe no. 60). The primers and probe for detecting the HTLV-1 *tax* mRNA load were used as described previously [8]. The primers and probe for IL-4 and IL-10 were used from TaqMan® Gene Expression Assays (IL-4: Hs: Hs00932431_m1, IL-10: Hs00174086_m1). Relative quantification of mRNA was performed using the comparative threshold cycle method using GAPDH as an endogenous control. For each sample, target gene expression was normalized to the expression of GAPDH. To determine the relative expression levels, the following formula was used: target gene expression $= 2^{-(Ct[target] - Ct[GAPDH])}$.

Proliferation assays

Separated PBMCs, PBMCs lacking $CD4^+CD25^+CCR4^+$ cells, PBMCs lacking $CD4^+CD25^-CCR4^-$ cells, $CD4^+CD25^+CCR4^+$ T cells, and $CD4^+CD25^-CCR4^-$ T cells from HAM/TSP patients were plated into 96-well round bottom plates (1×10^5 per well) without any mitogenic stimuli. RPMI 1640 with L-Glutamine (Wako, Japan) supplemented with 5% human AB serum (Gibco-Invitrogen, NY), penicillin, and streptomycin (Wako, Japan) was used as the culture medium. After 6 days of culture, 1 μCi tritium thymidine was added to each well, and the cells were cultured for an additional 16 hours. A liquid scintillation counter was used to measure the proliferation. Cultures were performed in triplicate for each experiment, and the average proliferation data was used for analysis.

Statistical analyses

The Wilcoxon signed-rank test was used to compare the HTLV-1 provirus load between $CD4^+CD25^+CCR4^+$ and $CD4^+CD25^+CCR4^-$ cells. An unpaired Student's *t* test was used to compare the frequency of $CD4^+CD25^+CCR4^+Foxp3^-$ T cells in PBMCs, to compare the percentage of the $Foxp3^+$ population in $CD4^+CD25^+CCR4^+$ T cells, to compare the frequency of $CD4^+CD25^-CCR4^-$, $CD4^+CD25^-CCR4^+$, $CD4^+CD25^+CCR4^-$ or $CD4^+CD25^+CCR4^+$ T cells, to compare the percentage of IFN-γ, IL-10 or IL-17 positive cells in each cell population, and to compare the magnitude of proliferation of $CD4^+CD25^+CCR4^+$ T cells between HDs and HAM/TSP patients. Paired Student's *t* test was used to compare the proliferative response of HAM PBMCs with and without $CD4^+CD25^+CCR4^+$ T cells and HAM PBMCs with and without $CD4^+CD25^-CCR4^-$ T cells, and to compare the proliferative response between $CD4^+CD25^+CCR4^+$ T cells and $CD4^+CD25^-CCR4^-$ T cells within HDs or HAM/TSP patients. The nonparametric Scheffe's test for multiple comparison was used to compare the data between HAM/TSP patients, ATL patients, and HDs. Spearman's rank correlation test was used to investigate the correlation between the percentage of IFN-γ-producing $CD4^+CD25^+CCR4^+$ T cells in PBMCs, HTLV-1 *tax* proviral load in PBMCs, clinical severity score, and concentration of neopterin in the CSF. Statistical analyses were performed using Statcel2 software.

Supporting Information

Figure S1 Purity of cell populations separated by FACS sorting. CD4+CD25−CCR4−, CD4+CD25−CCR4+, CD4+CD25+CCR4−, and CD4+CD25+CCR4+T cells were separated by FACS. The purity of each population was indicated as the histogram of fractions from (a)–(d): (a) CD4+CD25+CCR4−, (b) CD4+CD25+CCR4+, (c) CD4+CD25−CCR4−, and (d) CD4+CD25−CCR4+T cells. The purity of each population is approximately 99%.
Found at: doi:10.1371/journal.pone.0006517.s001 (0.60 MB TIF)

Figure S2 Schematic hypothesis outlining the importance of the different characteristics of HTLV-1-infected T cells in HAM/TSP and ATL patients. An imbalance in the THAM/Treg ratio in HTLV-1-infected CD4+CD25+CCR4+T cells may be an important factor that contributes to immunological differences of the host immune response between HAM/TSP and ATL.
Found at: doi:10.1371/journal.pone.0006517.s002 (0.34 MB TIF)

Acknowledgments

The authors would like to acknowledge the excellent technical assistance provided by Katsunori Takahashi, Yuko Ishikura, Yasuo Kunitomo and Ayako Une.

Author Contributions

Conceived and designed the experiments: YY NA. Performed the experiments: YY NA. Analyzed the data: YY NA. Contributed reagents/materials/analysis tools: YY NA TS AU KA DH TI HF SA NY RF. Wrote the paper: YY NA KN SJ TN. Reviewed and edited the manuscript: KN SJ TN.

References

1. Uchiyama T, Yodoi J, Sagawa K, Takatsuki K, Uchino H (1977) Adult T-cell leukemia: clinical and hematologic features of 16 cases. Blood 50: 481–492.
2. Kaplan JE, Osame M, Kubota H, Igata A, Nishitani H, et al. (1990) The risk of development of HTLV-1-associated myelopathy/tropical spastic paraparesis among persons infected with HTLV-1. J Acquir Immune Defic Syndr 3: 1096–1101.
3. Gessain A, Barin F, Vernant JC, Gout O, Maurs L, et al. (1985) Antibodies to human T-lymphotropic virus type-I in patients with tropical spastic paraparesis. Lancet 2: 407–410.
4. Osame M, Usuku K, Izumo S, Ijichi N, Amitani H, et al. (1986) HTLV-I associated myelopathy, a new clinical entity. Lancet 1: 1031–1032.
5. Nishioka K, Maruyama I, Sato K, Kitajima I, Nakajima Y, et al. (1989) Chronic inflammatory arthropathy associated with HTLV-I. Lancet 1: 441.
6. Nakagawa M, Izumo S, Ijichi S, Kubota H, Arimura K, et al. (1995) HTLV-I-associated myelopathy: analysis of 213 patients based on clinical features and laboratory findings. J Neurovirol 1: 50–61.
7. Jacobson S, Shida H, McFarlin DE, Fauci AS, Koenig S (1990) Circulating CD8+ cytotoxic T lymphocytes specific for HTLV-I pX in patients with HTLV-I associated neurological disease. Nature 348: 245–248.
8. Yamano Y, Nagai M, Brennan M, Mora CA, Soldan SS, et al. (2002) Correlation of human T-cell lymphotropic virus type 1 (HTLV-1) mRNA with proviral DNA load, virus-specific CD8(+) T cells, and disease severity in HTLV-1-associated myelopathy (HAM/TSP). Blood 99: 88–94.
9. Furuya T, Nakamura T, Fujimoto T, Nakane S, Kambara C, et al. (1999) Elevated levels of interleukin-12 and interferon-gamma in patients with human T lymphotropic virus type I-associated myelopathy. J Neuroimmunol 95: 185–189.
10. Izumo S, Umehara F, Kashio N, Kubota R, Sato E, et al. (1997) Neuropathology of HTLV-1-associated myelopathy (HAM/TSP). Leukemia 11 Suppl 3: 82–84.
11. Jacobson S (2002) Immunopathogenesis of human T cell lymphotropic virus type I-associated neurologic disease. J Infect Dis 186 Suppl 2: S187–192.
12. Yamano Y, Cohen CJ, Takenouchi N, Yao K, Tomaru U, et al. (2004) Increased expression of human T lymphocyte virus type I (HTLV-I) Tax11-19 peptide-human histocompatibility leukocyte antigen A*201 complexes on CD4+CD25+T cells detected by peptide-specific, major histocompatibility complex-restricted antibodies in patients with HTLV-I-associated neurologic disease. J Exp Med 199: 1367–1377.
13. Koyanagi Y, Itoyama Y, Nakamura N, Takamatsu K, Kira J, et al. (1993) In vivo infection of human T-cell leukemia virus type I in non-T cells. Virology 196: 25–33.
14. Nagai M, Brennan MB, Sakai JA, Mora CA, Jacobson S (2001) CD8(+) T cells are an in vivo reservoir for human T-cell lymphotropic virus type I. Blood 98: 1858–1861.
15. Jones KS, Petrow-Sadowski C, Huang YK, Bertolette DC, Ruscetti FW (2008) Cell-free HTLV-1 infects dendritic cells leading to transmission and transformation of CD4(+) T cells. Nat Med 14: 429–436.
16. Enose-Akahata Y, Oh U, Grant C, Jacobson S (2008) Retrovirally induced CTL degranulation mediated by IL-15 expression and infection of mononuclear phagocytes in patients with HTLV-I-associated neurologic disease. Blood 112: 2400–2410.
17. Sakaguchi S, Ono M, Setoguchi R, Yagi H, Hori S, et al. (2006) Foxp3+CD25+CD4+ natural regulatory T cells in dominant self-tolerance and autoimmune disease. Immunol Rev 212: 8–27.
18. Hori S, Nomura T, Sakaguchi S (2003) Control of regulatory T cell development by the transcription factor Foxp3. Science 299: 1057–1061.
19. Viglietta V, Baecher-Allan C, Weiner HL, Hafler DA (2004) Loss of functional suppression by CD4+CD25+ regulatory T cells in patients with multiple sclerosis. J Exp Med 199: 971–979.
20. Yamano Y, Takenouchi N, Li HC, Tomaru U, Yao K, et al. (2005) Virus-induced dysfunction of CD4+CD25+ T cells in patients with HTLV-I-associated neuroimmunological disease. J Clin Invest 115: 1361–1368.
21. Matsuoka M (2005) Human T-cell leukemia virus type I (HTLV-I) infection and the onset of adult T-cell leukemia (ATL). Retrovirology 2: 27.
22. Yoshie O, Fujisawa R, Nakayama T, Harasawa H, Tago H, et al. (2002) Frequent expression of CCR4 in adult T-cell leukemia and human T-cell leukemia virus type 1-transformed T cells. Blood 99: 1505–1511.
23. Acosta-Rodriguez EV, Rivino L, Geginat J, Jarrossay D, Gattorno M, et al. (2007) Surface phenotype and antigenic specificity of human interleukin 17-producing T helper memory cells. Nat Immunol 8: 639–646.
24. Hieshima K, Nagakubo D, Nakayama T, Shirakawa AK, Jin Z, et al. (2008) Tax-inducible production of CC chemokine ligand 22 by human T cell leukemia virus type 1 (HTLV-1)-infected T cells promotes preferential transmission of HTLV-1 to CCR4-expressing CD4+T cells. J Immunol 180: 931–939.
25. Okayama A, Stuver S, Matsuoka M, Ishizaki J, Tanaka G, et al. (2004) Role of HTLV-1 proviral DNA load and clonality in the development of adult T-cell leukemia/lymphoma in asymptomatic carriers. Int J Cancer 110: 621–625.
26. Yoshie O, Imai T, Nomiyama H (2001) Chemokines in immunity. Adv Immunol 78: 57–110.
27. Oh U, Grant C, Griffith C, Fugo K, Takenouchi N, et al. (2006) Reduced Foxp3 protein expression is associated with inflammatory disease during human t lymphotropic virus type 1 Infection. J Infect Dis 193: 1557–1566.
28. Hayashi D, Kubota R, Takenouchi N, Tanaka Y, Hirano R, et al. (2008) Reduced Foxp3 expression with increased cytomegalovirus-specific CTL in HTLV-I-associated myelopathy. J Neuroimmunol 200: 115–124.
29. Michaëlsson J, Barbosa HM, Jordan KA, Chapman JM, Brunialti MK, et al. (2008) The frequency of CD127low expressing CD4+CD25high T regulatory cells is inversely correlated with human T lymphotrophic virus type-1 (HTLV-1) proviral load in HTLV-1-infection and HTLV-1-associated myelopathy/tropical spastic paraparesis. BMC Immunol 9: 41.
30. Lee I, Wang L, Wells AD, Dorf ME, Ozkaynak E, et al. (2005) Recruitment of Foxp3+T regulatory cells mediating allograft tolerance depends on the CCR4 chemokine receptor. J Exp Med 201: 1037–1044.
31. Karube K, Ohshima K, Tsuchiya T, Yamaguchi T, Kawano R, et al. (2004) Expression of FoxP3, a key molecule in CD4CD25 regulatory T cells, in adult T-cell leukaemia/lymphoma cells. Br J Haematol 126: 81–84.
32. Hanon E, Goon P, Taylor GP, Hasegawa H, Tanaka Y, et al. (2001) High production of interferon gamma but not interleukin-2 by human T-lymphotropic virus type I-infected peripheral blood mononuclear cells. Blood 98: 721–726.
33. Nomoto M, Utatsu Y, Soejima Y, Osame M (1991) Neopterin in cerebrospinal fluid: a useful marker for diagnosis of HTLV-I-associated myelopathy/tropical spastic paraparesis. Neurology 41: 457.
34. Yoshida Y, Une F, Utatsu Y, Nomoto M, Furukawa Y, et al. (1999) Adenosine and neopterin levels in cerebrospinal fluid of patients with neurological disorders. Intern Med 38: 133–139.
35. Itoyama Y, Minato S, Kira J, Goto I, Sato H, et al. (1988) Spontaneous proliferation of peripheral blood lymphocytes increased in patients with HTLV-I-associated myelopathy. Neurology 38: 1302–1307.
36. Vine AM, Witkover AD, Lloyd AL, Jeffery KJ, Siddiqui A, et al. (2002) Polygenic control of human T lymphotropic virus type I (HTLV-I) provirus load and the risk of HTLV-I-associated myelopathy/tropical spastic paraparesis. J Infect Dis 186: 932–939.
37. Kohno T, Yamada Y, Akamatsu N, Kamihira S, Imaizumi Y, et al. (2005) Possible origin of adult T-cell leukemia/lymphoma cells from human T lymphotropic virus type-1-infected regulatory T cells. Cancer Sci 96: 527–533.
38. Nagai M, Kubota R, Greten TF, Schneck JP, Leist TP, et al. (2001) Increased activated human T cell lymphotropic virus type I (HTLV-I) Tax11-19-specific memory and effector CD8+ cells in patients with HTLV-I-associated myelopathy/tropical spastic paraparesis: correlation with HTLV-I provirus load. J Infect Dis 183: 197–205.
39. Kannagi M (2007) Immunologic control of human T-cell leukemia virus type I and adult T-cell leukemia. Int J Hematol 86: 113–117.
40. Kubota R, Nagai M, Kawanishi T, Osame M, Jacobson S (2000) Increased HTLV type 1 tax specific CD8+ cells in HTLV type 1-associated myelopathy/tropical spastic paraparesis: correlation with HTLV type 1 proviral load. AIDS Res Hum Retroviruses 16: 1705–1709.
41. Nagai M, Yamano Y, Brennan MB, Mora CA, Jacobson S (2001) Increased HTLV-I proviral load and preferential expansion of HTLV-I Tax-specific CD8+T cells in cerebrospinal fluid from patients with HAM/TSP. Ann Neurol 50: 807–812.
42. Chen S, Ishii N, Ine S, Ikeda S, Fujimura T, et al. (2006) Regulatory T cell-like activity of Foxp3+ adult T cell leukemia cells. Int Immunol 18: 269–277.
43. Wu Y, Borde M, Heissmeyer V, Feuerer M, Lapan AD, et al. (2006) FOXP3 controls regulatory T cell function through cooperation with NFAT. Cell 126: 375–387.
44. Shimizu Y, Takamori A, Utsunomiya A, Kurimura M, Yamano Y, et al. (2009) Impaired Tax-specific T-cell responses with insufficient control of HTLV-1 in a subgroup of individuals at asymptomatic and smoldering stages. Cancer Sci 100(3): 481–489.
45. Toulza F, Heaps A, Tanaka Y, Taylor GP, Bangham CR (2008) High frequency of CD4+Foxp3+ cells in HTLV-1 infection: inverse correlation with HTLV-1 specific CTL response. Blood 111(10): 5047–5053.
46. Shimoyama M (1991) Diagnostic criteria and classification of clinical subtypes of adult T-cell leukaemia-lymphoma. A report from the Lymphoma Study Group (1984-87). Br J Haematol 79: 428–437.

Severe loss of invariant NKT cells exhibiting anti–HTLV-1 activity in patients with HTLV-1–associated disorders

*Kazuko Azakami,[1,2] *Tomoo Sato,[1] Natsumi Araya,[1] Atae Utsunomiya,[3] Ryuji Kubota,[4] Kenshi Suzuki,[5] Daisuke Hasegawa,[1] Toshihiko Izumi,[1] Hidetoshi Fujita,[1] Satoko Aratani,[1] Ryoji Fujii,[1] Naoko Yagishita,[1] Hajime Kamijuku,[6] Takuro Kanekura,[2] Ken-ichiro Seino,[6] Kusuki Nishioka,[1] Toshihiro Nakajima,[7] and Yoshihisa Yamano[1]

[1]Department of Molecular Medical Science, Institute of Medical Science, St Marianna University School of Medicine, Kawasaki; [2]Department of Dermatology, Kagoshima University Graduate School of Medical and Dental Sciences, Kagoshima; [3]Department of Hematology, Imamura Bun-in Hospital, Kagoshima; [4]Center for Chronic Viral Diseases, Kagoshima University, Kagoshima; [5]Department of Hematology, Japanese Red Cross Medical Center, Tokyo; [6]Division of Bioregulation Research, Institute of Medical Science, St Marianna University School of Medicine, Kawasaki; and [7]St Marianna University School of Medicine, Kawasaki, Choju Medical Institute, Fukushimura Hospital, Toyohasi, and Misato Marine Hospital, Kochi, Japan

Invariant natural killer T (iNKT) cells are unique T cells that regulate the immune response to microbes, cancers, and autoimmunity. We assessed the characteristics of iNKT cells from persons infected with human T-lymphotropic virus type 1 (HTLV-1). Whereas most infected persons remain asymptomatic carriers (ACs) throughout their lives, a small proportion, usually with high equilibrium proviral loads, develop 2 diseases: HTLV-1–associated myelopathy/tropical spastic paraparesis (HAM/TSP) and adult T-cell leukemia (ATL). We demonstrated that the frequency of iNKT, NK, and dendritic cells in the peripheral blood of HAM/TSP and ATL patients is decreased. We also observed an inverse correlation between the iNKT cell frequency and the HTLV-1 proviral load in the peripheral blood of infected persons. Notably, in vitro stimulation of peripheral blood cells with α-galactosylceramide led to an increase in the iNKT cell number and a subsequent decrease in the HTLV-1–infected T-cell number in samples from ACs but not HAM/TSP or ATL patients. Our results suggest that iNKT cells contribute to the immune defense against HTLV-1, and iNKT-cell depletion plays an important role in the pathogenesis of HAM/TSP and ATL. Therefore, iNKT cell–based immunotherapy may be an effective strategy for preventing these HTLV-1–associated disorders. (Blood. 2009;114:3208-3215)

Introduction

Human T-cell lymphotropic virus type 1 (HTLV-1) causes persistent infection. Whereas most infected persons remain asymptomatic carriers (ACs), 3% to 5% develop a T-cell malignancy termed adult T-cell leukemia (ATL), and another 0.25% to 3% develop a chronic progressive inflammatory neurologic disease known as HTLV-1–associated myelopathy/tropical spastic paraparesis (HAM/TSP).[1-3] One of the most important pathogenic factors in HAM/TSP is an increased HTLV-1 load in the peripheral blood mononuclear cells (PBMCs) and cerebrospinal fluid,[4-6] which suggests that in affected persons, virus control is inadequate. A higher HTLV-1 load increases the risk of HAM/TSP and ATL.[4,7] Therefore, the precise mechanisms controlling HTLV-1–infected cells must be better understood. With regard to the host defense mechanisms involved in HTLV-1 infection, the role of HTLV-1–specific $CD8^+$ cytotoxic T lymphocytes (CTLs) has been studied.[8-10] The HTLV-1–specific CTL response is critical for a low viral load to be maintained.[9-11] Despite the high frequency of HTLV-1–specific CTLs, the number of HTLV-1–infected T cells is surprisingly high in HAM/TSP patients.[5,6] We and others have reported that the maturation and functioning of HTLV-1–specific CTLs are inadequate in HAM/TSP patients, although in vitro studies have shown that these CTLs exert cytolytic activity against HTLV-1–expressing target cells.[12,13] Therefore, we hypothesize that there may be another cell population without CTLs that contributes to the control of HTLV-1–infected T cells.

A unique T-cell subpopulation, natural killer T (NKT) cells, constitute a subset of lymphocytes that share the features of both innate and adaptive immune cells. Unlike conventional T cells, NKT cells express a T-cell receptor (TCR) that recognizes glycolipids instead of protein antigens. Moreover, these cells share properties and receptors with NK cells. They rapidly produce granzymes and perforins on stimulation. Among the $CD3^+$ T cells in human blood, 10% to 25% express NK cell–surface molecules, such as CD161, and these can be classified as NKT cells.[14,15] A small population of T cells within this NKT cell subset expresses a highly conserved Vα24Jα18 TCR chain that associates preferentially with Vβ11.[16-18] These T cells are referred to as invariant NKT (iNKT) cells. Very recently, a novel clonotypic monoclonal antibody 6B11 specific for the Vα24Jα18 TCR chain has been shown to selectively stain human iNKT cells.[18,19] Activation of human iNKT cells requires the presentation of glycolipids, such as α-galactosylceramide (α-GalCer) on the major histocompatibility complex class I–like molecule CD1d.[20] α-GalCer stimulation induces rapid cytokine production and potent antitumor and antipathogen responses by iNKT cells.[21-25] Human α-GalCer–stimulated iNKT cells also induce the rapid maturation of dendritic

Submitted February 2, 2009; accepted July 22, 2009. Prepublished online as *Blood* First Edition paper, August 7, 2009; DOI 10.1182/blood-2009-02-203042.

*K.A. and T.S. contributed equally to this work.

The online version of this article contains a data supplement.

The publication costs of this article were defrayed in part by page charge payment. Therefore, and solely to indicate this fact, this article is hereby marked "advertisement" in accordance with 18 USC section 1734.

cells (DCs) and activation of NK cells, thereby enhancing antitumor and antipathogen cytotoxicity.[24,26] Furthermore, one subset of DCs, myeloid DCs (mDCs), induces the activation of iNKT cells by increasing CD1d expression on their surface.[27] Another subset of DCs, plasmacytoid DCs (pDCs), secretes type1 interferon and supports mDCs in promoting iNKT cell activation.[28] Furthermore, activated iNKT cells also enhance acquired immunity. Thus, human iNKT cells bridge the innate and adaptive immune responses by interacting with both DCs and NK cells, and they play crucial roles in controlling viral infection and tumor cells.[29] Therefore, we investigated the frequency and activity of iNKT cells, NK cells, and DCs in HTLV-1–infected persons to determine whether iNKT cells have anti-HTLV-1 activity and play a pivotal role in the pathogenesis of HTLV-1–associated disorders.

We demonstrated that the frequency of iNKT cells, NK cells, and DCs is significantly decreased among PBMCs from HAM/TSP and ATL patients. We have also reported an inverse correlation between the frequency of iNKT cells and the proviral load in the PBMCs of HTLV-1–infected persons. We showed that in vitro α-GalCer stimulation of cells from ACs leads to an increase in the number of iNKT cells and that, after stimulation, the number of infected cells decreases. On the other hand, the number of iNKT cells among PBMCs from HAM/TSP and ATL patients did not increase on α-GalCer stimulation and, after stimulation, the number of infected cells did not decrease. Our results suggest that iNKT cells play a critical role in controlling HTLV-1 infection and that their activity is selectively depleted in both HAM/TSP and ATL patients.

Methods

Subjects and cell preparation

Written informed consent was obtained from all subjects before the study. The study complied with the tenets of the Declaration of Helsinki and was part of a clinical protocol reviewed and approved by the institutional ethics committee of each participating institution.

The study included 12 healthy donors (HDs; 5 men and 7 women; mean age, 55.64 years), 12 ACs (4 men and 8 women; mean age, 55.75 years), 13 HAM/TSP patients (3 men and 10 women; mean age, 58.15 years), and 11 ATL patients (3 with smoldering ATL and 8 with chronic ATL; 2 men and 9 women; mean age, 55.73 years). None of the subjects had comorbidities or had received prior immunosuppressive or cytotoxic chemotherapy. HAM/TSP was diagnosed according to the World Health Organization guidelines; ATL diagnosis was based on the criteria of Shimoyama.[30] HTLV-1 seropositivity was determined by the particle agglutination method (Serodia-HTLV-1; Fujirebio) and confirmed by Western blot (SRL Inc). Peripheral blood samples were collected; PBMCs were prepared by centrifugation over Ficoll-Hypaque gradients and viably cryopreserved in liquid nitrogen. Samples were collected at 3 different hospitals, numbered, and sent to our institute, after which they were processed equally. The investigators knew only the sample number and were unaware of the patient allocation. The identity of the allocated patient was shared only after the analysis.

Flow cytometric analysis

PBMCs were immunostained with various combinations of the following fluorescence-conjugated antibodies to cell surface markers: lineage cocktail (Lin 1) of monoclonal antibodies against CD3, CD14, CD16, CD19, CD20, and CD56 (BD Biosciences), anti–human leukocyte antigen (HLA)-DR (LN3; eBioscience), anti-CD123 (9F5; BD Biosciences), anti-CD11c (3.9; eBioscience), anti-CD3 (UCTH1; eBioscience), anti-CD16 (CB16; eBioscience), anti-CD56 (B159; BD Biosciences), anti-Vα24Jα18 (6B11; BD Biosciences), anti-CD4 (L3T4; eBioscience), anti-CD161 (DX12; BD Biosciences), anti-CD1d (51.1; eBioscience), anti-CD40 (5C3; eBioscience), anti-CD80 (2D10.4; eBioscience), anti-CD86 (IT2.2; eBioscience), anti-CD19 (HB19; eBioscience), anti-CD14 (61D3; eBioscience), and anti-HLA-ABC (W6/32; eBioscience). Each cell phenotype was defined as follows: mDC ($Lin^-HLA\text{-}DR^+CD11c^+$), pDC ($Lin^-HLA\text{-}DR^+CD123^+$), NK cells ($CD3^-CD16^+CD56^+$), $CD56^{bright}CD16^-$ NK cells ($CD3^-CD16^-CD56^{bright}$), and iNKT cells ($CD3^+V\alpha24J\alpha18^+$). Cells were stained with saturating concentrations of antibody (4°C, 30 minutes) in the dark and washed twice before analysis on a FACSCalibur (BD Biosciences). For perforin staining, cells were fixed and permeabilized with a staining buffer set (eBioscience) and intracellularly stained using a perforin reagent set (BD Biosciences). Data were processed using FlowJo software (TreeStar). For cell sorting, we used JSAN (BayBioscience), and the purity exceeded 95%.

Real-time PCR

The HTLV-1 proviral DNA load was measured using ABI Prism 7500 SDS (Applied Biosystems) as described previously.[6] Briefly, DNA was extracted, and 100-ng samples were analyzed per well. The proviral DNA load was calculated by the following formula: copy number of HTLV-1 (*pX*) per 100 cells = (copy number of *pX*)/(copy number of β actin/2) × 100.

α-GalCer stimulation of iNKT cells

PBMCs from HDs, ACs, and HAM/TSP and ATL patients were plated in 96-well round-bottom plates (10^5 cells per well) with or without 100 ng/mL α-GalCer (KRN7000; Funakoshi Co Ltd) in the presence or absence of 200 U/mL recombinant human interleukin-2 (IL-2; PeproTech) and cultured for 21 days. Cells were harvested for analysis on days 7, 14, and 21. RPMI-1640 with L-glutamine (Wako) supplemented with 10% fetal bovine serum (Invitrogen), 40 U/mL penicillin, and 40 μg/mL streptomycin (Wako) was used as the culture medium.

Statistical analysis

Nonparametric Scheffé F test was used for multiple comparisons of the frequency of iNKT and NK cells among the subject groups. Multiple comparisons of the mDC and pDC frequency among the subject groups were performed with the parametric Tukey-Kramer test. Scheffé F test was used for multiple comparisons of the expression levels of CD1d, CD86, and HLA-ABC among the subject groups. To assess the correlation between the HTLV-1 proviral load in PBMCs and DCs, Spearman rank correlation test was used to investigate the correlation between the frequency of iNKT cells, NK cells, and DCs and the proviral load in PBMCs. This test was also used to determine the correlation between the expression levels of the surface molecules (CD1d, CD86, and HLA-ABC) on and the proviral load in DCs. The proviral load in DCs of ACs and HAM/TSP patients and that after culture with or without α-GalCer stimulation was compared with the Wilcoxon signed-rank test. Statistical analyses were performed using the Statcel software, version 2 (OMS Publishing Inc).

Results

Decreased frequency of iNKT cells, NK cells, and DCs in PBMCs from HAM/TSP and ATL patients

To investigate the iNKT cell frequency in HTLV-1–infected persons, including HAM/TSP and ATL patients, we assayed the frequency of $CD3^+V\alpha24J\alpha18^+$ T cells in PBMCs from HDs (n = 12), ACs (n = 12), HAM/TSP patients (n = 13), and ATL patients (n = 11) using flow cytometry (Figure 1A-B). The percentage of iNKT cells among the total PBMCs was significantly decreased in HAM/TSP (0.00%-0.05%, mean = 0.0159%) and ATL patients (0.00%-0.04%, mean = 0.0150%) compared with that in HDs (0.01%-0.14%, mean = 0.0638%). The iNKT cell frequency in ACs (0.02%-0.14%, mean = 0.0525%) was lower than that in HDs and higher than that in HAM/TSP and ATL

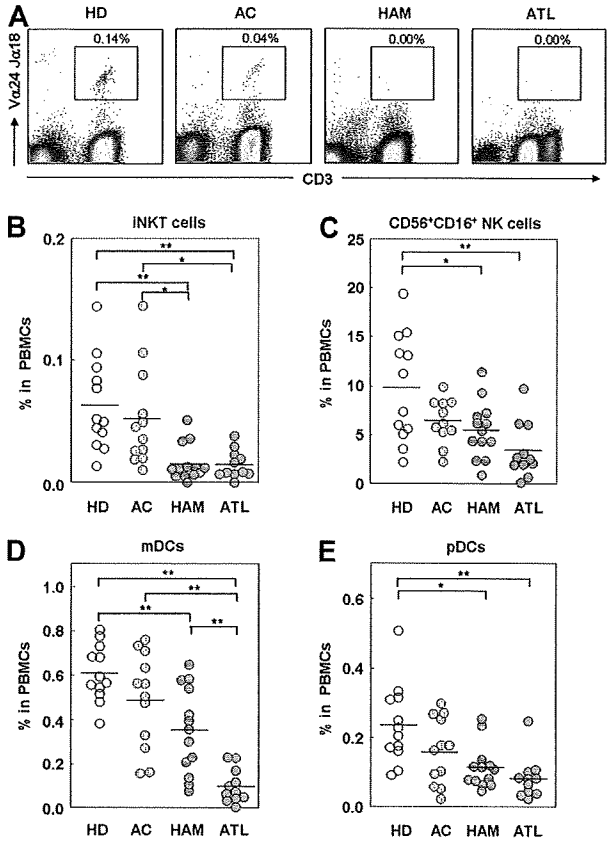

Figure 1. Decreased frequency of iNKT and NK cells, mDCs, and pDCs among PBMCs from HAM/TSP and ATL patients. (A) Representative FACS plot of iNKT cells from HDs, ACs, HAM/TSP patients (HAM), and ATL patients. PBMCs were stained for CD3 and Vα24Jα18, and the expression of CD3 and Vα24Jα18 is plotted. Numbers adjacent to the outlined area indicate the percentage of iNKT cells in total PBMCs. Plots of the frequency of iNKT cells (B), $CD56^+CD16^+$ NK cells (C), mDCs (D), and pDCs (E) among PBMCs from 12 HDs, 12 ACs, 13 HAM/TSP patients, and 11 ATL patients. The horizontal bar represents the mean value for each group. Scheffé F test was used for statistical analysis. Statistically significant differences: $^*P < .05$, $^{**}P < .01$.

patients (Figure 1B). Analysis of the frequency of NK cells ($CD3^-CD56^+CD16^+$) in the total PBMCs showed that the number of NK cells was lower in HAM/TSP and ATL patients than in HDs (Figure 1C). As in the case of iNKT cells, the frequency of NK cells in the ACs was lower than that in HDs but higher than that in HAM/TSP and ATL patients (Figure 1B). We also analyzed the frequency of $CD56^{bright}CD16^-$ NK cells, which were recently identified as cells with low cytotoxicity and inhibitory function for T-cell proliferation[31] (supplemental Figure 1, available on the *Blood* website; see the Supplemental Materials link at the top of the online article). The number of $CD56^{bright}CD16^-$ NK cells was lower in ATL patients than in HDs with no statistical significance; further, the number of these cells in the HAM/TSP patients and ACs was equivalent to that in HDs. Because DCs are crucial for the in vivo activation of iNKT cells,[27,32] we analyzed the frequency of 2 major peripheral blood subtypes of DCs (mDCs and pDCs) in the subjects (Figure 1D-E). The mDC frequency in HAM/TSP patients was lower than that in HDs ($P < .01$) and similar to that in ACs (Figure 1D). The mDC frequency was significantly lower in ATL patients than in HDs ($P < .01$), ACs ($P < .01$), and HAM/TSP patients ($P < .01$). The mDC frequency was lower in ACs than in HDs, although the difference was not statistically significant (Figure 1D). Furthermore, the pDC frequency was lower in both HAM/TSP and ATL patients than in HDs (Figure 1E). The pDC frequency was also lower in ACs than in HDs, but the difference was not statistically significant. To summarize, the frequency of cell subsets that play a role in innate immunity was lower in the HTLV-1–infected persons, especially HAM/TSP and ATL patients.

Inverse correlation between frequency of iNKT cells and proviral load in peripheral blood of HTLV-1–infected persons

To examine whether iNKT and NK cells, mDCs, and pDCs in HTLV-1–infected persons (Figure 1) contribute to the defense against HTLV-1, we assayed the correlation between the frequency of each cell population and the HTLV-1 proviral load as measured by quantitative real-time PCR of PBMCs from ACs (n = 12) and HAM/TSP patients (n = 13; Figure 2). As shown in Figure 2A, the frequency of iNKT cells was inversely and significantly correlated with the proviral load ($P = .008$ by Spearman rank correlation test); the frequency of NK cells ($P = .449$), mDCs ($P = .712$), and pDCs ($P = .894$) was not (Figure 2B-D). These results suggest that iNKT cells play an important role in the defense against HTLV-1.

Equivalent expression level of CD1d in all study groups

iNKT cells recognize their cognate antigen expressed on the major histocompatibility complex class I–like molecule CD1d, and mDCs induce the activation of iNKT cells by increasing surface CD1d expression.[27] Therefore, we examined whether the frequency of iNKT cells in HAM/TSP and ATL patients decreases because of the decreased expression of CD1d on mDCs. We analyzed CD1d expression on mDCs from 9 HDs, 7 ACs, 9 HAM/TSP patients, and 3 ATL patients using flow cytometry (Figure 3A). The CD1d expression level per mDC was similar among the study subjects. Because CD1d is also expressed on monocytes and B cells, we analyzed the CD1d expression level on the Lin^+ population (which includes monocytes and B cells) from the subjects. As shown in Figure 3B, the CD1d expression level per Lin^+ cell was also similar among the study subjects. We further analyzed the CD1d expression level on monocytes ($CD14^+$) and B cells ($CD19^+$) in PBMCs from 9 HDs, 4 ACs, 9 HAM/TSP patients, and 3 ATL patients using flow cytometry (supplemental Figure 2); the CD1d expression level per monocyte and B cell was equivalent among the subject groups.

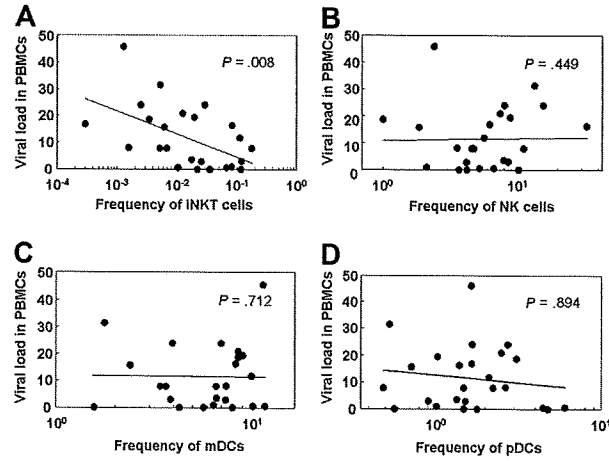

Figure 2. Inverse correlation between the frequency of iNKT cells and the proviral load in peripheral blood from HTLV-1–infected persons. The correlation between the HTLV-1 proviral load in PBMCs and the frequency of iNKT cells (A), $CD56^+CD16^+$ NK cells (B), mDCs (C), and pDCs (D) from HTLV-1–infected persons (ACs, n = 12; HAM/TSP patients, n = 13) was statistically analyzed using the Spearman rank correlation test.

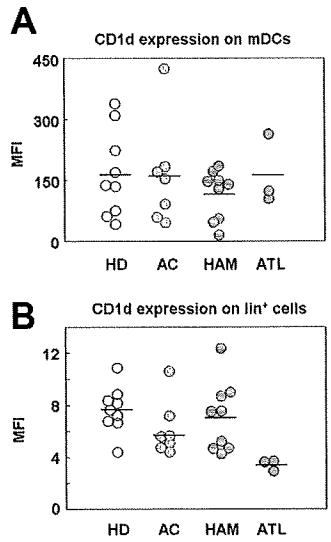

Figure 3. Equivalent expression levels of CD1d on mDCs and lineage-positive (Lin⁺) cells from HDs, ACs, and HAM/TSP patients, and ATL patients. Plots of the expression level (mean fluorescence intensity [MFI]) of CD1d molecules on mDCs (A) and Lin⁺ cells (B) among PBMCs from HDs (n = 9), ACs (n = 7), HAM/TSP patients (n = 9), and ATL patients (n = 3). The horizontal bar represents the mean value for each group. Statistical analysis of the expression level for each study subject revealed no statistically significant differences by 1-way analysis of variance and Scheffé F test.

pDCs cooperate with mDCs to promote antiviral activity by activating iNKT cells.[28,33] Therefore, we subsequently analyzed the surface expression level of DC-activation markers, such as CD40, CD80, CD86, and HLA-ABC on the mDCs and pDCs of 9 HDs, 7 ACs, 9 HAM/TSP patients, and 3 ATL patients (supplemental Figure 3). CD40 and CD80 expression on both circulating mDCs and pDCs (data not shown) and CD86 expression on pDCs (supplemental Figure 3A) were negligible in all subjects. CD86 expression on mDCs and HLA-ABC expression on mDCs and pDCs (supplemental Figure 3) were detectable in all subjects, but there was no statistically significant difference in the expression of either among the study subjects.

No correlation between the high HTLV-1 proviral load in DCs of HAM/TSP patients and CD1d expression level

HTLV-1 infects DCs,[34] and the extracellular HTLV-1 Tax protein has been reported to induce the overexpression of CD86 and decreased expression of HLA-ABC on DCs.[35] Moreover, human immunodeficiency virus type 1 (HIV-1) reportedly down-regulates CD1d expression.[36,37] We hypothesized that HTLV-1 infection of DCs may alter their function by affecting the expression level of CD1d, CD86, and HLA-ABC on the cell surface. Therefore, we first separated mDCs and pDCs from 5 ACs and 5 HAM/TSP patients by fluorescence-activated cell sorter (FACS) and quantified the HTLV-1 proviral load. As shown in Figure 4A, the proviral load was significantly higher in the mDCs of HAM/TSP patients than in those of ACs ($P = .038$). Moreover, it was also higher in the pDCs of HAM/TSP patients than in those of ACs (Figure 4A), although the difference was not statistically significant ($P = .053$). We analyzed the correlation between the proviral load in PBMCs and that in mDCs or pDCs and found a positive correlation (Figure 4B). Thus, in infected persons, in vivo HTLV-1 infection of mDCs and pDCs is apparent, and the proviral load in DCs is associated with the total proviral load in PBMCs.

To determine whether HTLV-1 infection of DCs affects CD1d expression on the DC surface, we analyzed the correlation between the proviral load in the mDCs and the expression level of CD1d on the mDCs of 8 HTLV-1–infected persons (3 ACs and 5 HAM/TSP patients). We observed no correlation (Figure 4C). Furthermore, we found no correlation between the proviral load in DCs and the expression levels of CD86 (Figure 4D) and HLA-ABC (Figure 4E). These results suggest that HTLV-1 infection of DCs has less effect on the expression levels of surface molecules important for the activation of T and iNKT cells.

Expansion of iNKT cells by in vitro α-GalCer stimulation can decrease the number of HTLV-1–infected T cells in ACs but not HAM/TSP and ATL patients

The inverse correlation between the frequency of iNKT cells and the proviral load in HTLV-1–infected persons (Figure 2A) suggests that iNKT cells play a role in the immune defense against HTLV-1. To explore whether iNKT cells have an anti–HTLV-1 effect, we cultured PBMCs from 6 ACs, 11 HAM/TSP patients, and 5 ATL patients with or without α-GalCer (100 ng/mL), and we analyzed the frequency of iNKT cells on days 0, 7, 14, and 21 using flow cytometry. As shown in Figure 5A, the number of iNKT cells in the

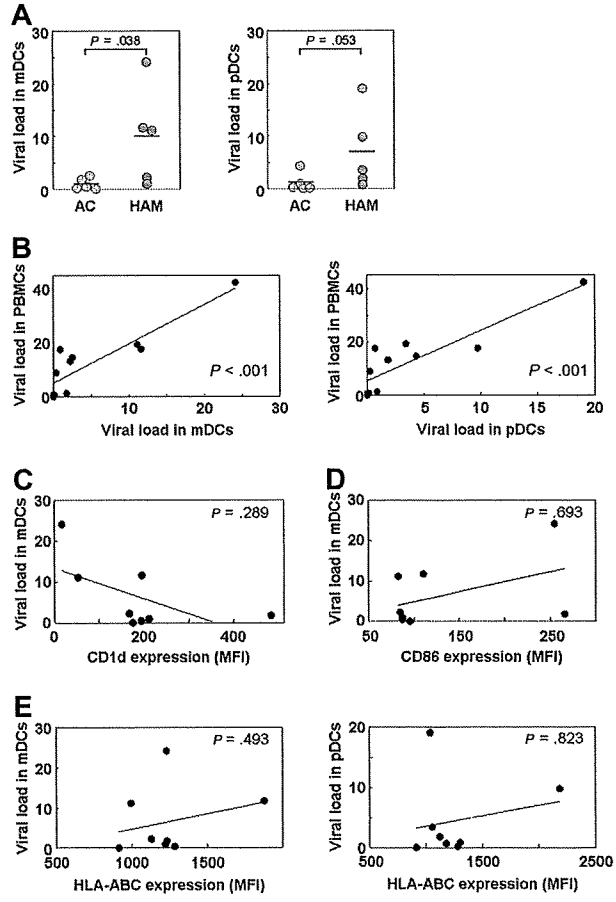

Figure 4. Increased HTLV-1 proviral load in DCs of HAM/TSP patients not associated with CD1d expression level. (A) The HTLV-1 proviral load was higher in mDCs ($P = .038$) and pDCs ($P = .053$) of HAM/TSP patients (n = 5) than in those of ACs (n = 5). The Mann-Whitney U test was used for statistical analysis. (B) Correlation analysis of the proviral load in PBMCs of HTLV-1–infected persons (5 ACs and 5 HAM/TSP patients) and that in mDCs ($P < .001$) and pDCs ($P < .001$) using Spearman rank correlation test. (C-E) No correlation was found between the proviral load in mDCs or pDCs of HTLV-1–infected persons (3 ACs and 5 HAM/TSP patients) and the expression level of CD1d on mDCs ($P = .289$; C), CD86 on mDCs ($P = .693$; D), and HLA-ABC on mDCs ($P = .493$) and pDCs ($P = .823$; E) by Spearman rank correlation test.

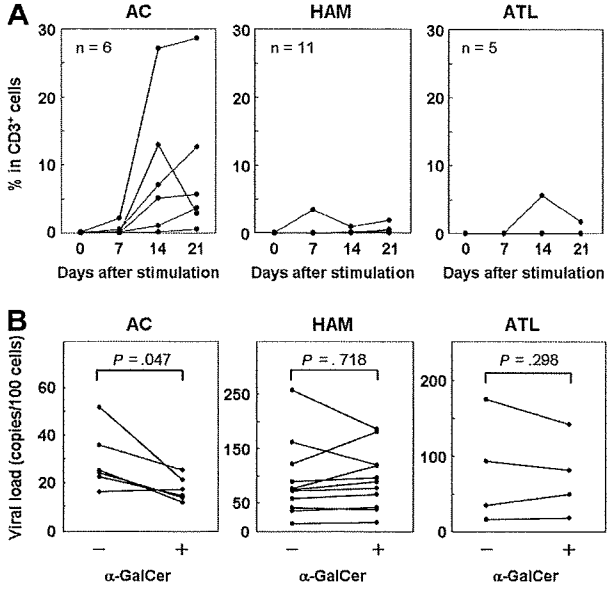

Figure 5. Expansion of iNKT cells by α-GalCer stimulation decreased the number of HTLV-1–infected T cells in ACs but not in HAM/TSP and ATL patients. (A) PBMCs from ACs (n = 6) and HAM/TSP (n = 11) and ATL patients (n = 5) were cultured with α-GalCer (100 ng/mL), and the percentage of iNKT cells on days 0, 7, 14, and 21 was plotted. (B) PBMCs from ACs (n = 6) and HAM/TSP (n = 11) and ATL patients (n = 4) were cultured for 14 days with or without α-GalCer, and the proviral load in each sample was quantified by real-time PCR. In ACs, the proviral load in PBMCs cultured with α-GalCer was significantly lower than that of cultured PBMCs grown without α-GalCer ($P = .047$). No significant difference was observed between HAM/TSP ($P = .718$) and ATL ($P = .298$) patients. Wilcoxon signed-rank test was used for statistical analysis.

PBMCs of most of the ACs increased after α-GalCer stimulation. On the other hand, the iNKT cells in the PBMCs from most of the HAM/TSP and ATL patients showed little or no response to α-GalCer stimulation.

Using real-time PCR, we also quantified the HTLV-1 proviral load in PBMCs from ACs (n = 6), HAM/TSP patients (n = 11), and ATL patients (n = 4) on day 14 of culture (Figure 5B). Notably, the proviral load in cultured PBMCs decreased ($P = .047$) only in samples from ACs, in which the number of iNKT cells increased on α-GalCer stimulation. However, in the samples from HAM/TSP and ATL patients, in which α-GalCer stimulation did not result in an increase in the number of iNKT cells, there was no difference in the proviral load of PBMCs grown in the presence or absence of α-GalCer.

iNKT cells functionally impaired in proliferation and perforin production are partially infected with HTLV-1 and CD4⁻ iNKT cells are depleted in HTLV-1–infected persons

The poor capacity of iNKT cells from HAM/TSP and ATL patients (Figure 5A) to expand in response to α-GalCer stimulation suggested 2 possibilities: (1) the frequency of iNKT cells before α-GalCer stimulation is low in these patients, as demonstrated in Figure 1, or (2) the proliferative response of iNKT cells in these patients is impaired. Although these possibilities are not mutually exclusive, to address whether iNKT cells of these patients have impaired proliferative response, we cultured PBMCs from 3 HDs, 3 ACs, 3 HAM/TSP patients, and 3 ATL patients, each with or without α-GalCer, and counted the absolute number of iNKT cells on days 0 and 14. We calculated the proliferative response ratio (absolute number of iNKT cells on day 14/absolute number of iNKT cells on day 0). As shown in Figure 6A, the proliferative response ratio of the iNKT cells was lower in HAM/TSP and ATL patients than in HDs and ACs. It was also lower in ACs than in HDs. Further, we examined whether this low response in HAM/TSP and ATL patients could be restored by IL-2, as has previously been reported in the case of cancer patients.[38] However, this was not possible (Figure 6A). Therefore, we conclude that the iNKT cells of patients with HTLV-1–associated disorders have impaired proliferation.

In assessing the characteristics of the iNKT cells of HTLV-1–infected persons, we were interested in not only their proliferative

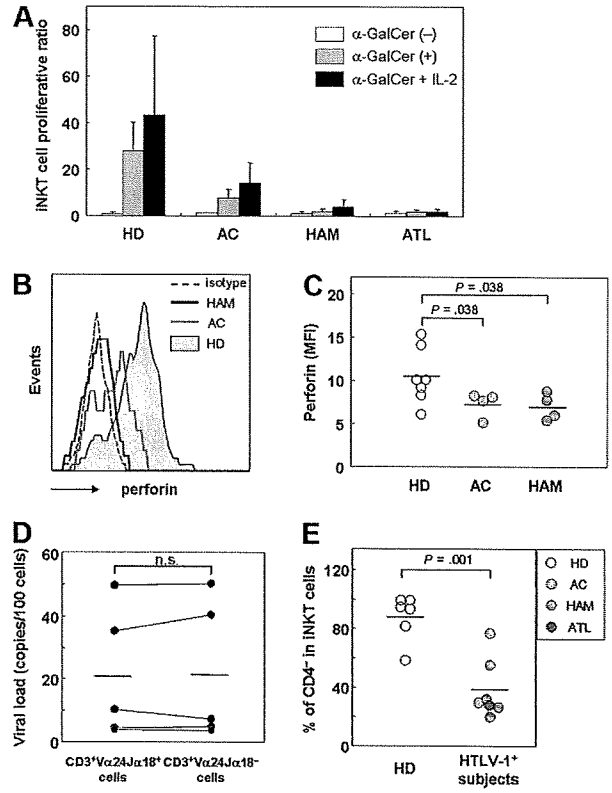

Figure 6. iNKT cells impaired in proliferation and perforin production are partially infected with HTLV-1 and CD4⁻ iNKT cells are depleted in HTLV-1–infected persons. (A) Proliferative response ratio of iNKT cells. PBMCs from HDs (n = 3), ACs (n = 3), and HAM/TSP (n = 3) and ATL patients (n = 3) were cultured without any treatment, with 100 ng/mL α-GalCer, or with α-GalCer (100 ng/mL) + IL-2 (100 U/mL). The fold change in the number of iNKT cells was calculated as the ratio of the absolute number of iNKT cells on day 14 divided by the absolute number of iNKT cells on day 0. Data are represented as mean ± SEM. (B) Representative FACS histogram of perforin expression by iNKT cells from HDs, ACs, and HAM/TSP patients. PBMCs were stained for perforin, Vα24Jα18, and CD3, and the expression levels of perforin in CD3⁺Vα24Jα18⁺ cells are plotted. (C) Levels of perforin expression (mean fluorescence intensity [MFI]) by CD3⁺Vα24Jα18⁺ iNKT cells of HDs, ACs, and HAM/TSP patients. PBMCs from 7 HDs, 4 ACs, and 6 HAM/TSP and 2 ATL patients were stained for perforin, Vα24Jα18, and CD3, and the expression level of perforin in each CD3⁺Vα24Jα18⁺ cell was plotted. In 2 of the 6 HAM/TSP patients and 2 ATL patients, perforin expression could not be analyzed because the frequency of iNKT cells was low. The perforin expression levels were lower in iNKT cells of ACs ($P = .038$), and HAM/TSP patients ($P = .038$) were lower than in those of HDs. The Mann-Whitney U test was used for statistical analysis. The horizontal bar represents the mean value of each group. (D) The HTLV-1 proviral load in CD3⁺Vα24Jα18⁺ (iNKT) cells and CD3⁺Vα24Jα18⁻ (CD3⁺ cells lacking iNKT cells) cells of 4 ACs and 1 HAM/TSP patient. Paired *t* test was used for statistical analysis; n.s. indicates not significant. (E) The percentage of CD4⁻ iNKT cells among total iNKT cells. PBMCs from 6 HDs and 7 HTLV-1–infected persons (1 AC, 5 HAM/TSP patients, and 1 ATL patient with detectable iNKT cells) were stained for CD3, CD4, and Vα24Jα18, the percentage of CD4⁺/CD4⁻ cells among CD3⁺Vα24Jα18⁺ iNKT cells was analyzed by FACS, and the percentage of CD4⁻ iNKT cells among total iNKT cells of each person was calculated. CD4⁻ iNKT cells were found to be dominantly depleted in HTLV-1–infected persons compared with HDs ($P = .001$ by Student *t* test).

capacity but also the expression levels of perforin, which is important for their cytotoxicity. We analyzed the expression levels of perforin in iNKT cells from 7 HDs, 4 ACs, and 4 HAM/TSP patients (none of the ATL patients and 4 of the 6 HAM/TSP patients could be analyzed because the frequency of iNKT cells was low). As shown in Figure 6B and C, the expression levels of perforin were lower in iNKT cells from ACs and HAM/TSP patients than in those from HDs, suggesting that the iNKT cells of HTLV-1–infected persons have lower cytotoxicity.

It has been reported that iNKT cells are highly susceptible to HIV-1 infection, and direct infection may be the primary cause of their low number and poor function.[39,40] Therefore, we analyzed HTLV-1 infection of iNKT cells from infected persons. Using PBMCs from 4 ACs and 1 HAM/TSP patient whose iNKT cell number was adequate for the assay, we separated $CD3^+V\alpha24J\alpha18^+$ (iNKT) and $CD3^+V\alpha24J\alpha18^-$ ($CD3^+$ cells without iNKT cells) cells by FACS and quantified the HTLV-1 proviral DNA load of each population by real-time PCR. As shown in Figure 6D, the proviral load in the iNKT cells (mean, 20.6 copies per 100 cells) was equivalent to that in the $CD3^+$ lacking iNKT cells (mean, 21.2 copies per 100 cells). Thus, HTLV-1 infection of iNKT cells was demonstrated. However, iNKT cells were not found to be more favorable targets of HTLV-1 infection than conventional T cells.

We were also interested in determining the ratio of $CD4^+$ and $CD4^-$ iNKT cells because it has been reported that the former may be more susceptible than the latter to HIV-1 infection and subsequent depletion[39,40] Therefore, we measured CD4 expression on $CD3^+V\alpha24J\alpha18^+$ iNKT cells from 6 HDs and 7 HTLV-1–infected persons (1 AC, 5 HAM/TSP patients, and 1 ATL patient with detectable iNKT cells). In the HTLV-1–infected persons, $CD4^-$ iNKT cells were notably more dominantly depleted than $CD4^+$ iNKT cells (Figure 6E).

Discussion

HTLV-1 causes 2 different diseases: HAM/TSP, a neuroimmunologic disorder, and ATL, a T-cell malignancy. Their common characteristic is the increased number of HTLV-1–infected cells (HTLV-1–infected leukemia cells in ATL).[4,7] Furthermore, the high viral load in ACs increases the risk of developing HAM/TSP or ATL.[4,7] These findings suggest that common mechanisms underlie the insufficient control of HTLV-1 infection in both diseases. iNKT cells have been implicated in infection control.[41-43] To test the hypothesis that iNKT cells may contribute to the immune defense against HTLV-1, we first measured the frequency of iNKT cells among PBMCs from the study groups. We demonstrated, for the first time, that the frequency of iNKT cells was significantly decreased in HTLV-1–infected persons, especially HAM/TSP or ATL patients (Figure 1).

To investigate the mechanisms underlying the decrease in iNKT cells in HTLV-1–infected persons, we measured the frequency of DCs and analyzed the expression levels of CD1d and activation markers (CD40, CD80, CD86, and HLA-ABC) on DCs from the study subjects because DCs are essential for the in vivo activation of iNKT cells[27,32] and mDCs induce activation by increasing the expression of CD1d on their cell surface.[27] As shown in Figure 1D and E, the DC frequency was decreased in patients with HTLV-1–associated disorders, especially ATL patients. The decreased frequency of DCs in ATL patients is consistent with a previous report.[44] We are the first to demonstrate the decreased DC frequency in HAM/TSP patients compared with HDs. Whereas the DC frequency in ATL patients was significantly lower, the expression level of CD1d on mDCs, monocytes, and B cells and that of activation markers (CD86 and HLA-ABC) on circulating DCs was similar among the study groups (Figure 3, supplemental Figure 3). These results suggest that the total number of CD1d-expressing mDCs and activated DCs is significantly decreased in ATL patients; this may be one of the mechanisms underlying the low frequency of iNKT cells in ATL patients. However, the total number of mDCs, and the expression level of CD1d and that of activation markers on mDCs, was equivalent between ACs and HAM/TSP patients (Figure 3), suggesting that the low number of iNKT cells in HAM/TSP patients is attributable to another mechanism.

Therefore, we next tested the hypothesis that HTLV-1 infection of DCs may result in the decreased frequency of iNKT cells, as has been reported for another human retrovirus, namely, HIV-1.[36,37] The HTLV-1 proviral load was significantly higher in DCs from HAM/TSP patients than from ACs (Figure 4). To determine the effect of HTLV-1 on CD1d expression and DC activation, we statistically analyzed the correlation between the proviral load in DCs and the expression level of CD1d and DC-activation markers. We found no correlation among the subjects (Figure 4). Although no statistical significance could be demonstrated, we observed a tendency toward an inverse correlation between the HTLV-1 proviral load in and the expression level of CD1d on mDCs (Figure 4C). Further in vitro studies are necessary to investigate the effect of HTLV-1 infection on CD1d expression on mDCs. Moreover, the absence of a correlation between the proviral load in DCs and the expression level of CD1d and activation markers on circulating DCs suggests other mechanisms by which HTLV-1 infection affects the functioning, maturation, and/or viability of DCs. HTLV-1–induced alterations in the DC function have been reported: Monocyte-derived DCs infected in vitro are poor stimulators of autologous T-cell differentiation.[45] Moreover, the ability of pDCs from ACs to produce type 1 interferon, an important antiviral mechanism of the innate immune system, is impaired.[44] Further studies must address the effect of HTLV-1 infection on DC functions, especially the function to activate iNKT cells.

Recently, it has been reported that iNKT cells are highly susceptible to HIV-1 infection, and direct infection may be a primary cause of their depletion and functional impairment.[39,40] Therefore, we quantified the rate of infection in iNKT cells in HTLV-1–infected persons to determine whether direct HTLV-1 infection is also an important mechanism underlying the decreased frequency and functional impairment of iNKT cells in such persons. As shown in Figure 6D, HTLV-1 was shown to infect iNKT cells to the same extent as conventional $CD3^+$ T cells, suggesting that iNKT cells are partially but not selectively infected with HTLV-1. However, we cannot exclude the possibility that HTLV-1 can induce iNKT cell depletion through direct infection. Therefore, we next compared the frequency of $CD4^+$ and $CD4^-$ iNKT cells between HDs and HTLV-1–infected persons (Figure 6E). Because HTLV-1 is known to preferentially infect $CD4^+$ cells over $CD4^-$ cells,[46] we hypothesized that the number of $CD4^+$ iNKT cells might be preferentially decreased if direct HTLV-1 infection of iNKT cells causes their depletion, as has been reported in the case of HIV-1.[39,40] However, contrary to our expectations, we clearly found that $CD4^-$ iNKT cells were selectively depleted in HTLV-1–infected persons, especially HAM/TSP and ATL patients (Figure 6E). These results suggest that direct HTLV-1 infection of iNKT cells is not the main cause of their depletion in infected persons. Recently, it has been reported that $CD4^-$ iNKT cells preferentially induce the Th1 response and are more important than

$CD4^+$ iNKT cells in controlling viral infection and cancers.[47,48] The predominant depletion of $CD4^-$ iNKT cells in HAM/TSP and ATL patients (Figure 6E) may contribute to the common underlying mechanisms of insufficient control of HTLV-1 infection in both diseases.

iNKT cells are known to exhibit antiviral activity.[49] We demonstrated an inverse correlation between the iNKT cell frequency and proviral load in the peripheral blood of HTLV-1–infected persons (Figure 2). In vitro stimulation of PBMCs by α-GalCer resulted in a decrease in the number of HTLV-1–infected T cells only in ACs, in whom the number of iNKT cells increased on α-GalCer stimulation (Figure 5). These results suggest that iNKT cells possess anti–HTLV-1 activity. There was no decrease in the proviral load in α-GalCer–stimulated PBMCs from HAM/TSP and ATL patients, in whom the number of iNKT cells did not increase on stimulation (Figure 5). This result further confirms the anti–HTLV-1 effect of iNKT cells. Moreover, iNKT cells in these patients may be functionally defective, as indicated by their low proliferative response on α-GalCer stimulation and low perforin production (Figure 6A). Because iNKT cells play a crucial role in DC- and NK-cell activation,[29] the decreased number and the functional impairment of iNKT cells in HAM/TSP and ATL patients may be one cause of the decreased frequency of DCs and NK cells (Figure 1) in these patients. Thus, iNKT depletion in HAM/TSP and ATL patients directly and/or indirectly diminishes the immune defense against HTLV-1, resulting in the insufficient control of HTLV-1–infected cells, including leukemia cells, in patients with HTLV-1–associated disorders.

CD1d-restricted iNKT cells play an important role to protect infection as well as to control tumor immunity and to regulate the deleterious immune responses in autoimmune diseases.[50] Therefore, the decreased frequency of iNKT cells in patients with HAM/TSP and ATL may underlie not only insufficient infected cell control but also the pathogenesis of ATL and HAM/TSP. Currently, evidence is accumulating about the potential use of iNKT-mediated immunotherapy as a clinical modulator in cancer and autoimmune disorders. iNKT cell–based immunotherapy using α-GalCer–loaded DCs can induce more efficient iNKT–cell activation; it has been well tolerated in clinical trials and effectively produces antitumor cytotoxic effects, leading to prolonged stable disease in some patients.[51] Furthermore, α-GalCer–loaded tumor cells have recently been shown to induce the activation of iNKT cells and NK cells more efficiently.[27] Moreover, IL-10–treated tolerogenic DCs can induce the regulatory function of iNKT cells, which enables them to control autoimmune diseases by suppressing deleterious immune responses.[52] These findings indicate the potential usefulness of immunotherapy targeting iNKT cells as one of the clinical therapeutic strategies for treating ATL and HAM/TSP. However, iNKT cells in HAM/TSP and ATL patients demonstrated poor proliferation on in vitro α-GalCer stimulation (Figures 5-6). This impaired proliferation could not be restored by IL-2, as has been successful in some cancers[38] (Figure 6A). These results suggest severe functional impairment of such iNKT cells. Therefore, α-GalCer–based therapy as a clinical modulator in HAM/TSP and ATL patients will be challenging. On the other hand, although the iNKT cells of ACs produced less perforin than those of HDs (Figure 6), the decreased proviral load after expansion of the iNKT cells by in vitro α-GalCer stimulation in ACs suggests that immunotherapy targeting iNKT cells will be potentially useful as a clinical therapeutic strategy to prevent HTLV-1–associated disorders.

In conclusion, this report highlights the ability of iNKT cells to reduce the HTLV-1 viral load in infected persons and suggests the importance of these cells in the pathogenesis of HAM/TSP and ATL. Our findings provide a platform to explore the potential use of α-GalCer as an immune modulator to prevent and/or treat HTLV-1–associated disorders. Studies on the implications of the loss of iNKT-cell subsets in the pathogenesis of HTLV-1 infection and associated diseases are underway in our laboratory.

Acknowledgments

The authors thank K. Takahashi, Y. Ishikura, Y. Kunitomo, and A. Une for technical assistance and Dr K. Arimura and members of the Department of Neurology and Geriatrics, Kagoshima University Graduate School of Medical and Dental Sciences, for useful support.

This work was supported in part by the Japan Society for the Promotion of Science (Grant-in Aid for Scientific Research); the Ministry of Education, Culture, Sports, Science and Technology, Japanese Ministry of Health, Labour, and Welfare (H21-NANCHI-IPPAN-008); National Institute of Biomedical Innovation; Uehara Memorial Foundation; Nagao Takeshi Nanbyo Foundation; Kanagawa Nanbyo Foundation; Mishima Kaiun Memorial Foundation; Takeda Science Foundation; ITSUU Laboratory Research Foundation; Kanae Foundation for Life and Socio-Medical Science; Japan Research Foundation for Clinical Pharmacology; Kanagawa Academy of Science and Technology (research grants); Japan College of Rheumatology; Nakajima Foundation; Osaka Foundation for Cancer Research; New Energy and Industrial Technology Development Organization; Mochida Pharmaceutical Company Ltd; Kanagawa High-Technology Foundation; Kanto Bureau of Economy, Trade and Industry; Mitsui Life Insurance Company Ltd; Heiwa Nakajima Foundation; Sagawa Foundation for Promotion of Cancer Research; and Tokyo Biochemical Research Foundation.

Authorship

Contribution: K.A. and T.S. performed the experiments and data analysis and wrote the manuscript; Y.Y. developed the project, performed the experiments and data analysis, and wrote the manuscript; N.A., A.U., R.K., K.S., D.H., T.I., H.F., S.A., R.F., N.Y., and H.K. contributed to sample collection and preparation; and A.U., R.K., T.K., K.S., K.N., and T.N. reviewed and edited the manuscript.

Conflict-of-interest disclosure: The authors declare no competing financial interests.

Correspondence: Yoshihisa Yamano, Department of Molecular Medical Science, Institute of Medical Science, St Marianna University School of Medicine, 2-16-1 Sugao, Miyamae-ku, Kawasaki, Kanagawa 216-8512, Japan; e-mail: yyamano@marianna-u.ac.jp.

References

1. Uchiyama T, Yodoi J, Sagawa K, Takatsuki K, Uchino H. Adult T-cell leukemia: clinical and hematologic features of 16 cases. *Blood.* 1977;50(3):481-492.
2. Gessain A, Barin F, Vernant JC, et al. Antibodies to human T-lymphotropic virus type-I in patients with tropical spastic paraparesis. *Lancet.* 1985; 2(8452):407-410.
3. Osame M, Usuku K, Izumo S, et al. HTLV-I associated myelopathy, a new clinical entity. *Lancet.* 1986;1(8488):1031-1032.
4. Nagai M, Usuku K, Matsumoto W, et al. Analysis of HTLV-I proviral load in 202 HAM/TSP patients and 243 asymptomatic HTLV-I carriers: high proviral load strongly predisposes to HAM/TSP. *J Neurovirol.* 1998;4(6):586-593.

5. Nagai M, Yamano Y, Brennan MB, Mora CA, Jacobson S. Increased HTLV-I proviral load and preferential expansion of HTLV-I Tax-specific CD8+ T cells in cerebrospinal fluid from patients with HAM/TSP. *Ann Neurol.* 2001;50(6):807-812.
6. Yamano Y, Nagai M, Brennan M, et al. Correlation of human T-cell lymphotropic virus type 1 (HTLV-1) mRNA with proviral DNA load, virus-specific CD8(+) T cells, and disease severity in HTLV-1–associated myelopathy (HAM/TSP). *Blood.* 2002;99(1):88-94.
7. Okayama A, Stuver S, Matsuoka M, et al. Role of HTLV-1 proviral DNA load and clonality in the development of adult T-cell leukemia/lymphoma in asymptomatic carriers. *Int J Cancer.* 2004;110(4): 621-625.
8. Jacobson S. Immunopathogenesis of human T cell lymphotropic virus type I-associated neurologic disease. *J Infect Dis.* 2002;186[suppl 2]:S187-S192.
9. Kannagi M. Immunologic control of human T-cell leukemia virus type I and adult T-cell leukemia. *Int J Hematol.* 2007;86(2):113-117.
10. Bangham CR. HTLV-1 infection: role of CTL efficiency. *Blood.* 2008;112(6):2176-2177.
11. Harashima N, Kurihara K, Utsunomiya A, et al. Graft-versus-Tax response in adult T-cell leukemia patients after hematopoietic stem cell transplantation. *Cancer Res.* 2004;64(1):391-399.
12. Tomaru U, Yamano Y, Nagai M, et al. Detection of virus-specific T cells and CD8+ T-cell epitopes by acquisition of peptide-HLA-GFP complexes: analysis of T-cell phenotype and function in chronic viral infections. *Nat Med.* 2003;9(4):469-476.
13. Sabouri AH, Usuku K, Hayashi D, et al. Impaired function of human T-lymphotropic virus type 1 (HTLV-1)-specific CD8+ T cells in HTLV-1–associated neurologic disease. *Blood.* 2008; 112(6):2411-2420.
14. Lanier LL, Chang C, Phillips JH. Human NKR-P1A: a disulfide-linked homodimer of the C-type lectin superfamily expressed by a subset of NK and T lymphocytes. *J Immunol.* 1994;153(6): 2417-2428.
15. Prussin C, Foster B. TCR V alpha 24 and V beta 11 coexpression defines a human NK1 T cell analog containing a unique Th0 subpopulation. *J Immunol.* 1997;159(12):5862-5870.
16. Porcelli S, Yockey CE, Brenner MB, Balk SP. Analysis of T cell antigen receptor (TCR) expression by human peripheral blood CD4-8-alpha/beta T cells demonstrates preferential use of several V beta genes and an invariant TCR alpha chain. *J Exp Med.* 1993;178(1):1-16.
17. Dellabona P, Padovan E, Casorati G, Brockhaus M, Lanzavecchia A. An invariant V alpha 24-J alpha Q/V beta 11 T cell receptor is expressed in all individuals by clonally expanded CD4-8- T cells. *J Exp Med.* 1994;180(3):1171-1176.
18. Exley MA, Hou R, Shaulov A, et al. Selective activation, expansion, and monitoring of human iNKT cells with a monoclonal antibody specific for the TCR alpha-chain CDR3 loop. *Eur J Immunol.* 2008;38(6):1756-1766.
19. Montoya CJ, Pollard D, Martinson J, et al. Characterization of human invariant natural killer T subsets in health and disease using a novel invariant natural killer T cell-clonotypic monoclonal antibody, 6B11. *Immunology.* 2007;122(1):1-14.
20. Wu DY, Segal NH, Sidobre S, Kronenberg M, Chapman PB. Cross-presentation of disialoganglioside GD3 to natural killer T cells. *J Exp Med.* 2003;198(1):173-181.
21. Kawano T, Nakayama T, Kamada N, et al. Antitumor cytotoxicity mediated by ligand-activated human V alpha24 NKT cells. *Cancer Res.* 1999; 59(20):5102-5105.
22. Nicol A, Nieda M, Koezuka Y, et al. Human invariant valpha24+ natural killer T cells activated by alpha-galactosylceramide (KRN7000) have cytotoxic anti-tumour activity through mechanisms distinct from T cells and natural killer cells. *Immunology.* 2000;99(2):229-234.
23. Takahashi T, Nieda M, Koezuka Y, et al. Analysis of human V alpha 24+ CD4+ NKT cells activated by alpha-glycosylceramide-pulsed monocyte-derived dendritic cells. *J Immunol.* 2000;164(9): 4458-4464.
24. Metelitsa LS, Naidenko OV, Kant A, et al. Human NKT cells mediate antitumor cytotoxicity directly by recognizing target cell CD1d with bound ligand or indirectly by producing IL-2 to activate NK cells. *J Immunol.* 2001;167(6):3114-3122.
25. Nieda M, Nicol A, Koezuka Y, et al. TRAIL expression by activated human CD4(+)V alpha 24NKT cells induces in vitro and in vivo apoptosis of human acute myeloid leukemia cells. *Blood.* 2001; 97(7):2067-2074.
26. Ishihara S, Nieda M, Kitayama J, et al. Alpha-glycosylceramides enhance the antitumor cytotoxicity of hepatic lymphocytes obtained from cancer patients by activating CD3-CD56+ NK cells in vitro. *J Immunol.* 2000;165(3):1659-1664.
27. Fujii S. Exploiting dendritic cells and natural killer T cells in immunotherapy against malignancies. *Trends Immunol.* 2008;29(5):242-249.
28. Raftery MJ, Winau F, Giese T, Kaufmann SH, Schaible UE, Schonrich G. Viral danger signals control CD1d de novo synthesis and NKT cell activation. *Eur J Immunol.* 2008;38(3):668-679.
29. Cerundolo V, Silk JD, Masri SH, Salio M. Harnessing invariant NKT cells in vaccination strategies. *Nat Rev Immunol.* 2009;9(1):28-38.
30. Shimoyama M. Diagnostic criteria and classification of clinical subtypes of adult T-cell leukaemia-lymphoma: a report from the Lymphoma Study Group (1984-87). *Br J Haematol.* 1991;79(3):428-437.
31. Poli A, Michel T, Theresine M, Andres E, Hentges F, Zimmer J. CD56bright natural killer (NK) cells: an important NK cell subset. *Immunology.* 2009; 126(4):458-465.
32. Hermans IF, Silk JD, Gileadi U, et al. NKT cells enhance CD4+ and CD8+ T cell responses to soluble antigen in vivo through direct interaction with dendritic cells. *J Immunol.* 2003;171(10): 5140-5147.
33. Montoya CJ, Jie HB, Al-Harthi L, et al. Activation of plasmacytoid dendritic cells with TLR9 agonists initiates invariant NKT cell-mediated cross-talk with myeloid dendritic cells. *J Immunol.* 2006; 177(2):1028-1039.
34. Jones KS, Petrow-Sadowski C, Huang YK, Bertolette DC, Ruscetti FW. Cell-free HTLV-1 infects dendritic cells leading to transmission and transformation of CD4(+) T cells. *Nat Med.* 2008; 14(4):429-436.
35. Mostoller K, Norbury CC, Jain P, Wigdahl B. Human T-cell leukemia virus type I Tax induces the expression of dendritic cell markers associated with maturation and activation. *J Neurovirol.* 2004;10(6):358-371.
36. Chen N, McCarthy C, Drakesmith H, et al. HIV-1 down-regulates the expression of CD1d via Nef. *Eur J Immunol.* 2006;36(2):278-286.
37. Li D, Xu XN. NKT cells in HIV-1 infection. *Cell Res.* 2008;18(8):817-822.
38. Yanagisawa K, Seino K, Ishikawa Y, Nozue M, Todoroki T, Fukao K. Impaired proliferative response of V alpha 24 NKT cells from cancer patients against alpha-galactosylceramide. *J Immunol.* 2002;168(12):6494-6499.
39. Motsinger A, Haas DW, Stanic AK, Van Kaer L, Joyce S, Unutmaz D. CD1d-restricted human natural killer T cells are highly susceptible to human immunodeficiency virus 1 infection. *J Exp Med.* 2002;195(7):869-879.
40. Sandberg JK, Fast NM, Palacios EH, et al. Selective loss of innate CD4(+) V alpha 24 natural killer T cells in human immunodeficiency virus infection. *J Virol.* 2002;76(15):7528-7534.
41. Kawano T, Cui J, Koezuka Y, et al. CD1d-restricted and TCR-mediated activation of valpha14 NKT cells by glycosylceramides. *Science.* 1997;278(5343): 1626-1629.
42. Seino K, Taniguchi M. Functional roles of NKT cell in the immune system. *Front Biosci.* 2004;9: 2577-2587.
43. Kronenberg M. Toward an understanding of NKT cell biology: progress and paradoxes. *Annu Rev Immunol.* 2005;23:877-900.
44. Hishizawa M, Imada K, Kitawaki T, Ueda M, Kadowaki N, Uchiyama T. Depletion and impaired interferon-alpha-producing capacity of blood plasmacytoid dendritic cells in human T-cell leukaemia virus type I-infected individuals. *Br J Haematol.* 2004;125(5):568-575.
45. Makino M, Wakamatsu S, Shimokubo S, Arima N, Baba M. Production of functionally deficient dendritic cells from HTLV-I-infected monocytes: implications for the dendritic cell defect in adult T cell leukemia. *Virology.* 2000;274(1):140-148.
46. Richardson JH, Edwards AJ, Cruickshank JK, Rudge P, Dalgleish AG. In vivo cellular tropism of human T-cell leukemia virus type 1. *J Virol.* 1990; 64(11):5682-5687.
47. Kim CH, Butcher EC, Johnston B. Distinct subsets of human Valpha24-invariant NKT cells: cytokine responses and chemokine receptor expression. *Trends Immunol.* 2002;23(11):516-519.
48. Bricard G, Cesson V, Devevre E, et al. Enrichment of human CD4+ V(alpha)24/Vbeta11 invariant NKT cells in intrahepatic malignant tumors. *J Immunol.* 2009;182(8):5140-5151.
49. Tupin E, Kinjo Y, Kronenberg M. The unique role of natural killer T cells in the response to microorganisms. *Nat Rev Microbiol.* 2007;5(6):405-417.
50. Seino K, Taniguchi M. Functionally distinct NKT cell subsets and subtypes. *J Exp Med.* 2005; 202(12):1623-1626.
51. Ishikawa A, Motohashi S, Ishikawa E, et al. A phase I study of alpha-galactosylceramide (KRN7000)-pulsed dendritic cells in patients with advanced and recurrent non-small cell lung cancer. *Clin Cancer Res.* 2005;11(5):1910-1917.
52. Yamaura A, Hotta C, Nakazawa M, Van Kaer L, Minami M. Human invariant Valpha24$^+$ natural killer T cells acquire regulatory functions by interacting with IL-10–treated dendritic cells. *Blood.* 2008;111(8):4254-4263.

J Neuropathol Exp Neurol

Vol. 68, No. 2
February 2009
pp. 199–209

ORIGINAL ARTICLE

Reduced Expression of Excitatory Amino Acid Transporter 2 and Diffuse Microglial Activation in the Cerebral Cortex in AIDS Cases With or Without HIV Encephalitis

Hui Qin Xing, MD, PhD, Hitoshi Hayakawa, MD, PhD, Ellen Gelpi, MD, PhD, Ryuji Kubota, MD, PhD, Herbert Budka, MD, PhD, and Shuji Izumo, MD, PhD

Abstract

To determine the relationship between the human immunodeficiency virus type 1 (HIV-1) encephalitis (HIVE) and diffuse poliodystrophy in the acquired immunodeficiency syndrome dementia complex, we examined the neuropathologic features in brain autopsy tissue specimens of HIV-1–infected patients with (n = 11) or without HIVE (n = 9). The brains were free of opportunistic diseases and major cerebrovascular lesions. In both groups, there was diffuse microglial activation, astrocytic gliosis, and decreased excitatory amino acid transporter 2 (EAAT-2) immunoreactivity. These changes did not correlate either with the severity of encephalitis or local HIV-1 infection as detected by p24 immunostaining. Some activated microglia expressed EAAT-2; interleukin-1β and tumor necrosis factor were detected only in microglial nodules of HIVE cases but not in areas with diffusely activated microglia. There was a significant negative correlation between the areas of EAAT-2 expression and numbers of activated microglia ($p < 0.01$) in cases with decreased EAAT-2. These data indicate that diffuse cortical changes may occur independently of HIVE in acquired immunodeficiency syndrome patients. The expression of EAAT-2 by activated microglia suggests that they might exert a compensatory effect that protects neurons from glutamate neurotoxicity.

Key Words: Astrocytes, Cerebral cortex, Excitatory amino acid transporter2, HIV encephalopathy, Immunohistochemistry, Microglia, Neuroprotection.

From the Division of Molecular Pathology, Center for Chronic Viral Diseases, Graduate School of Medical and Dental Sciences, Kagoshima University, Kagoshima (HQX, HH, RK, SI), Japan; and Institute of Neurology, Medical University Vienna (HH, EG, HB), Vienna, Austria.

Send correspondence and reprint requests to: Shuji Izumo, MD, PhD, Division of Molecular Pathology, Center for Chronic Viral Diseases, Graduate School of Medical and Dental Sciences, Kagoshima University, 8-35-1, Sakuragaoka, Kagoshima 890-8544, Japan; E-mail: izumo@m.kufm.kagoshima-u.ac.jp

This work was supported by AIDS research grants of the Health Sciences Research Grants (H15-AIDS-004) from the Japan Ministry of Health, Labour, and Welfare, and Grants-in-Aid for Scientific Research from the Japan Society for the Promotion of Science.

INTRODUCTION

The acquired immunodeficiency syndrome (AIDS) dementia complex (ADC) is characterized by diffuse and nodular inflammatory infiltrates and multinucleated giant cells (MNGCs) with myelin pallor and axonal damage in brain white matter. Its pathological substrate is termed *human immunodeficiency virus encephalitis* (HIVE) (1–8), in which abundant HIV-infected macrophages and microglial cells can be demonstrated. However, poor correlations between the clinical manifestations of brain dysfunction and these pathological findings have been repeatedly noted (9, 10). On the other hand, neuronal damage, as indicated by atrophy of the cerebral cortex (7), neuronal loss (11–13), neuron apoptosis (14), and synaptic and dendritic simplification (15–17) in the cerebral cortex are additional histopathologic features of ADC that have been termed *diffuse poliodystrophy* (DPD) (3, 7). The precise relationships between these histopathologic patterns (i.e. the inflammatory process in the white matter and degenerative process in the cortex) are unclear, in part, because of the complexity of histopathologic findings in human autopsy brains.

In the simian immunodeficiency virus (SIV)–infected macaque model, we previously demonstrated that an inflammatory process with virus-infected MNGCs in the white matter and degenerative changes of the cerebral cortex along with development of immunodeficiency can occur independently according to the cell tropism of inoculated viruses (18). Further analysis of the frontal cortex of macaques with advanced AIDS demonstrated astrocytic abnormalities such as apoptosis and decreased expression of excitatory amino acid transporter 2 (EAAT-2) and alternative expression of EAAT-2 by diffusely activated microglial cells; the latter finding suggests a neuroprotective role for activated microglia. Virus-infected cells and SIV encephalitis could not be found in and around such cortical lesions (19), suggesting that astrocytic degeneration and microglial activation might play a role in the pathogenesis of AIDS dementia independently of the development of HIVE.

To determine whether similar changes occur in HIV-1–infected brains, we examined autopsy specimens from HIV-1–infected individuals, particularly focusing on microglial activation, apoptosis, and EAAT-2 expression, as

well as the localization of HIVE, using various immunohistochemical methods.

MATERIALS AND METHODS

Case Material

Among autopsy cases at the Institute of Neurology, Medical University of Vienna, since 1983, there have been 429 patients who died from HIV-1 infection. The records of these cases were screened, and those who had opportunistic infections or neoplasm in the brain and those with massive cerebrovascular lesions were excluded from this analysis. Twenty cases were selected (Table); 11 had HIVE and 9 had no apparent histopathologic changes in the brain. These patients had died between 1987 and 2002; only 5 patients had died before 1991, before highly active antiretroviral therapy became available. Brain sections of 2 autopsy cases from patients with amyotrophic lateral sclerosis were used as controls. These patients did not show any clinical and histopathologic brain abnormalities other than the pyramidal tract involvement. Paraffin sections of the frontal lobe and pons were processed for further histopathologic examination.

Histopathologic Examination

The histopathologic methods used in this study have been described elsewhere (18). We used various immunohistochemical stains for detecting activated microglia and astrocyte abnormalities and virus-infected cells. Brain tissue specimens were embedded in paraffin, sectioned, and mounted on glass slides. The EnVision system (DAKO, Carpinteria, CA) was used for the immunohistochemical staining, except for the guinea pig anti-glial glutamate transporter 1, EAAT-2 antibody, with which the avidin-biotin-peroxidase complex method (Vector, Burlingame, CA) was applied. Immunoreactivity was visualized using either diaminobenzidine peroxidase (brown) or the 3-amino-9-ethylcarbazole substrate-chromogen system (DAKO; red). Light counterstaining was done with hematoxylin.

Antibodies

To identify activated microglia, we used mouse monoclonal antibody to human macrophage CD68 (KP1, 1:50; DAKO, Glostrup, Denmark) and rabbit anti-ionized calcium-binding adaptor molecule-1 (Iba1) antibody (1:500; Wako Chemicals, Osaka, Japan). To characterize astrocyte abnormalities, we used guinea pig anti-glial glutamate transporter-1, EAAT-2 antibody (1:6000; Chemicon, Temecula, CA). For HIV-infected cells, we used mouse anti–HIV-1 p24 antibody (1:10, DakoCytomation, Kyoto, Japan).

Mouse anti-human Ki-67 antibody (1:300; DAKO), which detects cells in all active phases of the cell cycle (i.e. G1, S, G2, and M), was used to detect dividing cells; sections of tonsil were used as positive controls. Mouse anti–human tumor necrosis factor (TNF) antibody (1:400; Abcam,

TABLE. Semiquantitative Assessment of Histopathologic Alterations

Patient No.	Diagnosis	Decrease of EAAT-2	Apoptosis		Diffuse Increase of Microglia		Ki-67	Gliosis	HIV p24	
			Cerebral Cortex	White Matter	Frontal Cortex	Pons	Cerebral Cortex		Cerebral Cortex	White Matter
1	HIVE	3	0	0	2	1	2	1	0	2
2	HIVE	3	1	2	3	1	2	0	1	0
3	HIVE	2	2	1	3	1	1	2	0	1
4	HIVE	2	1	1	1	1	1	0	0	1
5	HIVE	2	2	1	3	1	2	3	0	1
6	HIVE	2	1	2	2	1	1	2	1	3
7	HIVE	1	2	1	1	1	1	3	2	2
8	HIVE	0	2	1	1	1	1	0	1	1
9	HIVE	0	1	3	1	1	1	3	0	3
10	HIVE	0	3	2	0	1	1	0	0	1
11	HIVE	0	2	2	0	1	1	0	0	1
12	No HIVE	3	0	0	3	3	3	0	0	0
13	No HIVE	3	1	1	3	3	1	2	0	0
14	No HIVE	3	1	1	0	1	1	0	0	0
15	No HIVE	2	0	0	2	1	1	0	0	0
16	No HIVE	1	2	1	0	1	1	0	0	0
17	No HIVE	0	0	0	2	1	1	0	0	0
18	No HIVE	0	0	0	3	3	1	2	0	0
19	No HIVE	0	0	0	3	1	1	1	0	0
20	No HIVE	0	1	1	3	3	3	0	0	0
21	ALS	0	0	0	0	nd	1	2	nd	nd
22	ALS	0	1	1	0	nd	1	0	nd	nd

ALS, amyotrophic lateral sclerosis control cases; EAAT-2, excitatory amino acid transporter 2; HIV, human immunodeficiency virus; HIVE, HIV encephalitis; No HIVE, HIV-1–positive cases without HIVE; nd, not determined.

Cambridge, MA) and rabbit polyclonal antibody to interleukin 1β (IL-1β, 1:200; Santa Cruz Biotechnology, Santa Cruz, CA) were used to detect the respective cytokines. A tonsil with chronic inflammation was used as a positive control. We also performed glial fibrillary acidic protein (GFAP), ubiquitin carboxyl-terminal esterase L1, and CD20 immunohistochemical staining for routine cell characterization.

Double Label Immunohistochemistry

To determine the phenotype of apoptotic cells, we performed double label immunohistochemistry for GFAP or CD68 using the EnVision system (DAKO) and for single-stranded DNA (ssDNA) using the avidin-biotin-alkaline phosphatase complex method (Vector); double labeling was performed with diaminobenzidine peroxidase followed by Vector blue alkaline phosphatase. To examine the phenotype of EAAT-2–positive cells, we performed double label immunohistochemistry for Iba1 and EAAT-2 using the same method.

To determine the phenotype of proliferating cells, double label immunohistochemistry was first performed for Iba1 or GFAP using the avidin-biotin-alkaline phosphatase complex method and then for Ki-67 using the EnVision system. Double labeling was performed using Vector blue alkaline phosphatase followed by the 3-amino-9-ethylcarbazole substrate-chromogen system.

Apoptosis

In situ terminal deoxynucleotidyl transferase 2′-deoxyuridine 5′-triphosphate–mediated nick end labeling (TUNEL) of fragmented DNA was done using an ApopTag in situ apoptosis detection kit (Chemicon). We also performed immunohistochemistry using affinity-purified polyclonal rabbit immunoglobulin G directed specifically against the active form of caspase 3 (1:1000; R&D Systems, Minneapolis, MN) and anti-ssDNA antibody (1:250; DakoCytomation) to identify apoptotic cells. Sections of tonsil were used as positive controls.

Quantitative Analysis of EAAT-2 Expression and Iba1 Microglial Activation

Five red-green-blue images of light microscopic pictures (original magnification: 100×) were randomly acquired from the second to the fifth layers of the frontal cortex stained with EAAT-2 using a Sony digital camera system. These red-green-blue images were converted to blue-subtracted images using Adobe Photoshop to obtain better contrast; EAAT-2–positive areas (pixels) were measured by the National Institutes of Health Image analysis program.

Iba1 antibody–positive cells were counted in 5 light microscopic fields (original magnification: 200×) of the second to the fifth cortical layers of the middle frontal gyrus. When more than 600 Iba1-positive cells were counted, this was considered evidence of an increase in the activated microglia. We also performed semiquantitative assessments for the immunohistochemical assessment of astrocytic gliosis, Ki-67– or CD68-positive cells, and TNF and IL-1β expression.

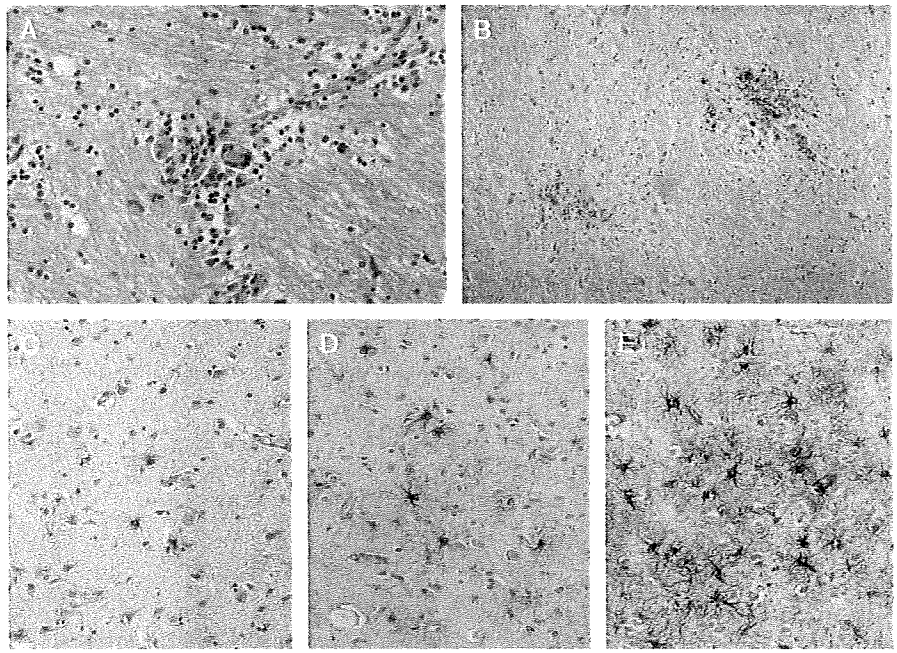

FIGURE 1. Pathological features in the brain specimens from human immunodeficiency virus (HIV)–infected cases. **(A)** Patient 6. The frontal cortex white matter shows perivascular inflammation and multinucleated giant cells (hematoxylin and eosin, original magnification: 100×). **(B)** Patient 6. Some HIV-immunopositive cells are detected in the glial nodule and perivascular infiltrates, anti-HIV p24 immunohistochemistry (original magnification: 40×). **(C–E)** Grading of astrocytic gliosis of the frontal cortex evaluated by anti-glial fibrillary acidic protein immunostaining (original magnification: 200×): mild (**C**, Patient 1 with HIV encephalitis [HIVE]), moderate (**D**, Patient 13 without HIVE), and marked (**E**, Patient 7 with HIVE).

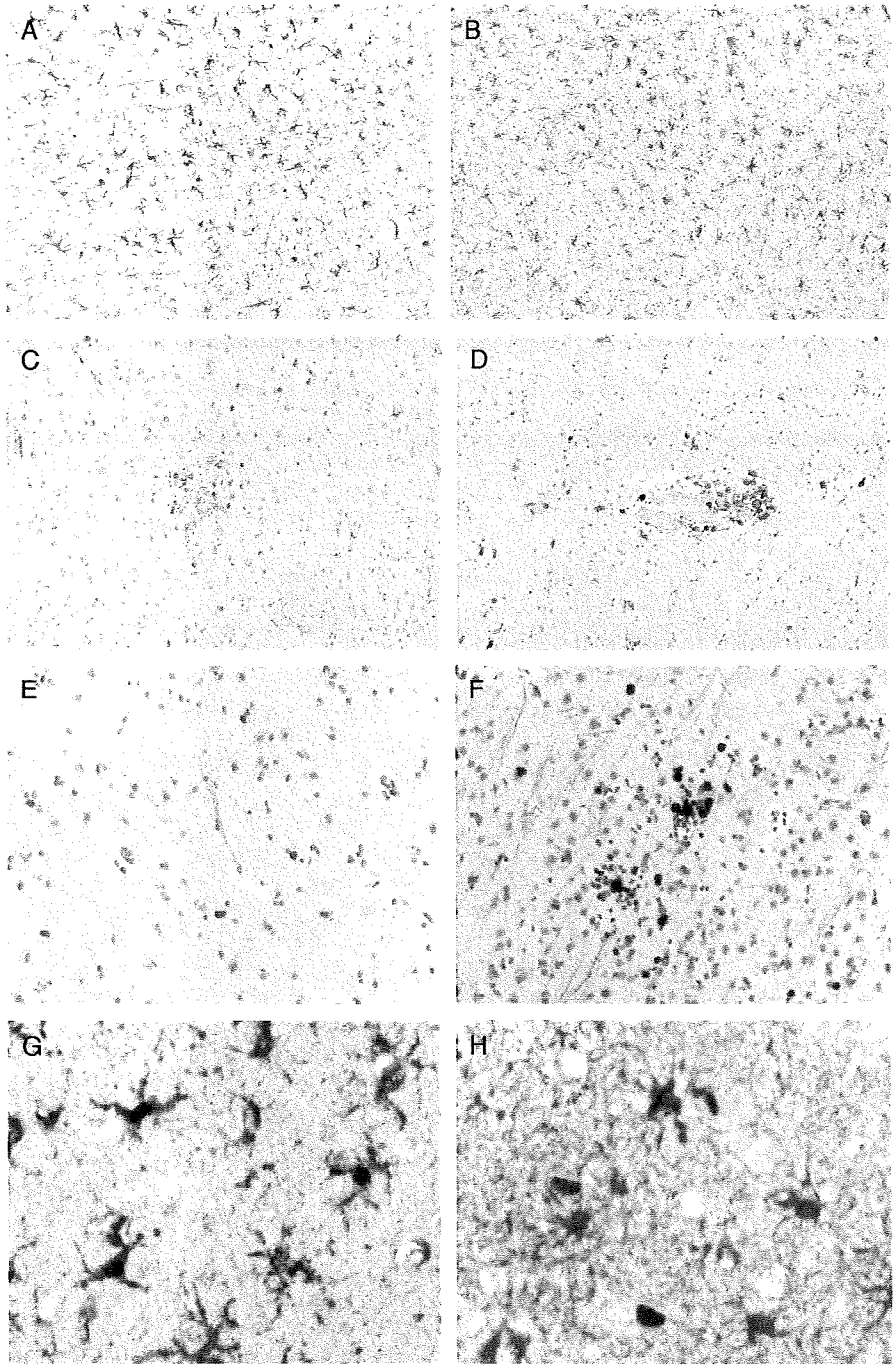

FIGURE 2. Increase and activation of microglia in the cerebral cortex and pons. **(A–D)** Anti-Iba1 immunostaining (original magnification: 200×). Patient 12 without human immunodeficiency virus 1 encephalitis (HIVE) shows diffuse microglial activation in the frontal cortex **(A)** and in the pons **(B)**. On the other hand, Patient 7 with HIVE in the cortex **(C)** and pons **(D)** shows localized Iba1-positive cells in perivascular infiltrates but no diffuse microglial activation. **(E)** Ki-67–positive proliferating cells are randomly distributed in the frontal cortex of Patient 12 without HIVE (original magnification: 200×). **(F)** Ki-67–positive proliferating cells are localized in the microglial nodules of the frontal cortex of Patient 7 with HIVE (original magnification: 200×). **(G)** Double label immunohistochemistry with anti-Iba1 (blue) and anti–Ki-67 (red) of the frontal cortex of Patient 12 without HIVE. Proliferating cells were also Iba1-positive microglial cells (original magnification: 200×). **(H)** Double label immunohistochemistry of anti-glial fibrillary acidic protein ([GFAP] blue) and anti–Ki-67 of the frontal cortex of Patient 12 without HIVE. Proliferating cells were not GFAP-positive astrocytes (original magnification: 400×).

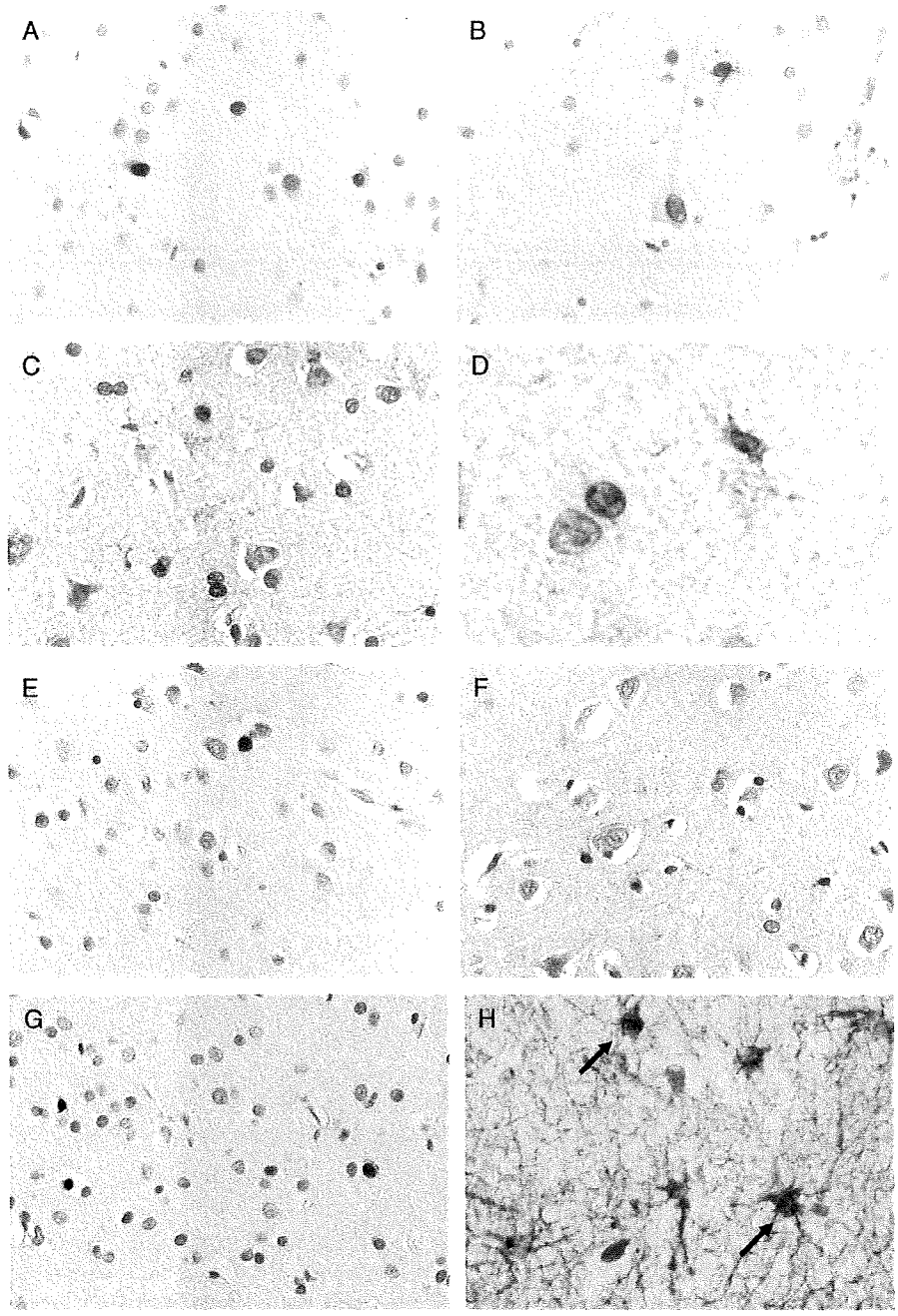

FIGURE 3. Apoptosis of glial cells and neurons in the frontal cortex. **(A–D)** Patient 10 with human immunodeficiency virus 1 encephalitis (HIVE). Scattered positive glial cells and neurons are demonstrated in the second layer (**[A]** original magnification: 400×) and the fifth layer (**[B]** original magnification: 400×) by ApopTag in situ. By anti–activated caspase 3 immunostaining, scattered positive cells are also detected in the second layer (**[C]** original magnification: 400×) and the fifth layer of the cortex (**[D]** original magnification: 800×). **(E, F)** Patient 16 without HIVE. Some positive glial cells are demonstrated in the second layer (**[E]** ApopTag in situ, original magnification: 400×) and the fifth layer (**[F]** anti–activated caspase 3, original magnification: 400×). **(G, H)** Patient 5 with HIVE. Scattered positive glial cells are demonstrated in the second layer (**[G]** anti–single-stranded DNA [ssDNA], original magnification: 200×), and some of ssDNA-positive cells were glial fibrillary acidic protein (GFAP) positive by double label with anti-GFAP (brown) and anti-ssDNA (blue) (**[H]** original magnification: 400×).

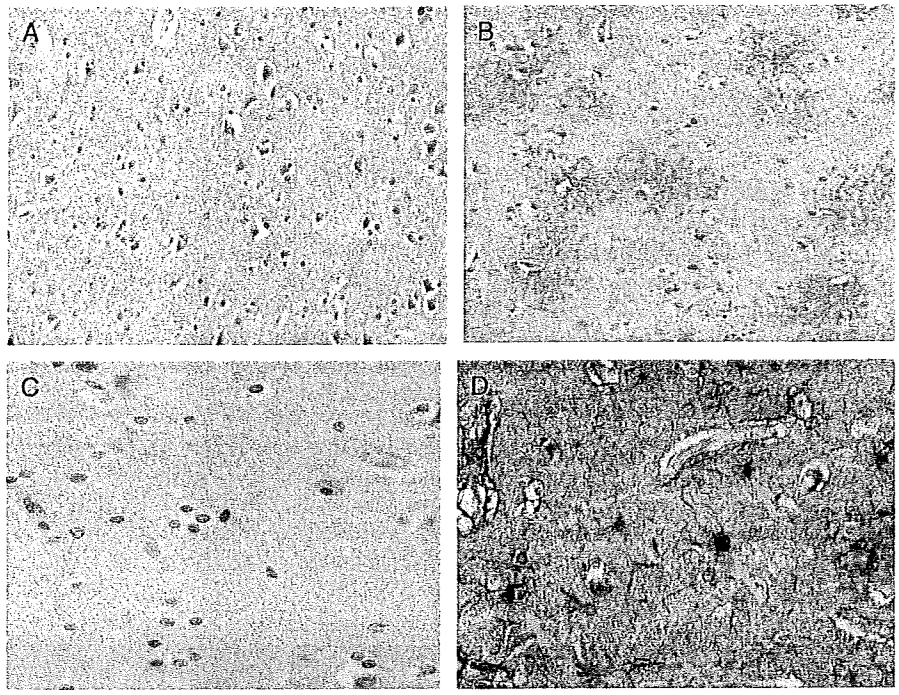

FIGURE 4. Decreased excitatory amino acid transporter 2 (EAAT-2) immunostaining and EAAT-2 staining in microglia in the cerebral cortex. **(A–C)** Anti–EAAT-2 immunostaining. Representative patterns of normal staining **([A]** Patient 11, original magnification: 200×), moderately decreased staining **([B]** Patient 15, original magnification: 200×), and markedly decreased staining **([C]** Patient 12, original magnification: 200×) are shown. **(D)** The EAAT-2 immunopositivity of microglia (arrows) by double label of anti-Iba1 (brown) and anti–EAAT-2 (dark blue) immunostaining (Patient 12, original magnification: 200×).

Statistical Analysis

Statistical significance was determined using commercial software (StatView for Windows; SAS Institute, Cary, NC). We analyzed the correlation between areas of EAAT-2 expression and numbers of Iba1-positive activated microglia in the frontal cortex.

RESULTS

Routine Histopathologic Examination

The pathological diagnosis of HIVE was suspected when either perivascular infiltration and MNGCs were present or it was present along with microglial nodules; the diagnosis was confirmed by positive HIV-1 p24 immunohistochemistry. Of the 20 brain tissue specimens from HIV-1–infected cases, 11 showed the features of HIVE including microglial nodules and perivascular infiltration with MNGCs in the frontal white matter (Fig. 1A) and pons (Fig. 1B). Microglial nodules were mainly composed of CD68-positive macrophages/microglia, and ubiquitin carboxyl-terminal esterase L1–positive T cells were scattered in the surrounding areas (not shown).

Immunohistochemical staining with anti–HIV-1 p24 antibody was positive in the macrophages/microglia and MNGCs of the inflammatory foci (Fig. 1B) and in a few perivascular macrophages of noninflamed areas in the white matter. Diffuse or focal astrocytic gliosis was detected in the frontal cortex of 5 cases with HIVE (Figs. 1C, E). In the 9 cases without HIVE or any other coexisting pathological lesion, we did not detect HIV-1–infected cells by HIV-1 p24 immunohistochemical staining; of these cases, diffuse or focal astrocytic gliosis was observed in the frontal cortex of 5 cases (Fig. 1D).

Activated Microglia in the Frontal Cortex and Pons

Iba1-positive microglial cells could be identified by their extended branches. Fewer than 300 immunopositive cells in 5 fields (original magnification: 200×) were counted in the 2 control amyotrophic lateral sclerosis cases. Of the 20 brain tissue specimens from the HIV-1–infected cases, 12 showed a diffuse increase of Iba1-positive microglia; that is, more than 600 positive cells in 5 fields in the frontal cortex (Fig. 2A). Of these 12 cases, 5 had HIVE (5/11, 45.5%), and 7 did not have HIVE (7/9, 77.8%); 4 of the 7 cases without HIVE also showed diffuse microglial activation in the pons (Fig. 2B). On the other hand, diffuse activation of microglia was not detected in the other 6 cases with HIVE or in 2 cases without HIVE; in these cases, Iba1-positive cells were restricted in their localization to the microglial nodules in the frontal cortex (Fig. 2C) and in perivascular infiltrates in the pons (Fig. 2D).

Ki-67–positive cells were randomly distributed in the frontal cortex in cases with diffuse microglial activation (Fig. 2E), whereas positively stained cells were localized in the microglial nodules in the cases with HIVE (Fig. 2F).

Some Iba1-positive microglia were also Ki-67 positive by double label immunohistochemistry (Fig. 2G). Ki-67–positive cells were not observed among the GFAP-positive astrocytes by double label immunohistochemistry with anti-GFAP and anti–Ki-67 antibodies (Fig. 2H).

Apoptosis of Glial Cells and Neurons in the Frontal Cortex in Cases With or Without HIVE

We used the in situ TUNEL method and immunohistochemical staining for the active form of caspase 3 and ssDNA to detect apoptosis. We found that 14 of the 20 HIV-1–infected cases, 10 with and 4 without HIVE, showed apoptosis of glial cells and/or neurons. In cases with HIVE, TUNEL-positive cells were mainly demonstrated in the second layer of the cortex and seemed to be both cell types (Fig. 3A). In the fifth layer of the cortex, positive labeling was also demonstrated in some large pyramidal neurons (Fig. 3B). In the activated caspase 3 staining, positive cells showed intracytoplasmic and nuclear labeling, and most of them seemed to be glial cells (Figs. 3C, D). Similar patterns of TUNEL-positive cells (Fig. 3E) and caspase 3 staining (Fig. 3F) were also observed in the cases without HIVE. The ssDNA-positive cells seemed to be small neuronal and glial cells (Fig. 3G). Some of the ssDNA-positive cells were also positive for GFAP by double label immunohistochemistry (Fig. 3H, arrows).

Reduction of EAAT-2 Expression in the Neuropil of the Frontal Cortex

The EAAT-2 was predominantly detected in the neuropil of the cerebral cortex; this is consistent with astrocytic expression of EAAT-2. The EAAT-2–positive areas were 70% to 76% (169,765–183,612 pixels) of the total area (240,975 pixels) in the control brain samples. In the HIV-1–infected cases, 8 cases showed more than 70% EAAT-2–positive areas (Fig. 4A). The other 12 cases showed less than 70% EAAT-2–positive areas; for example, 30% of the area was stained in Patient 15 (Fig. 4B), and 6% was stained in Patient 12 (Fig. 4C). Of the cases with reduced EAAT-2 staining, 7 had HIVE and 5 did not. In addition,

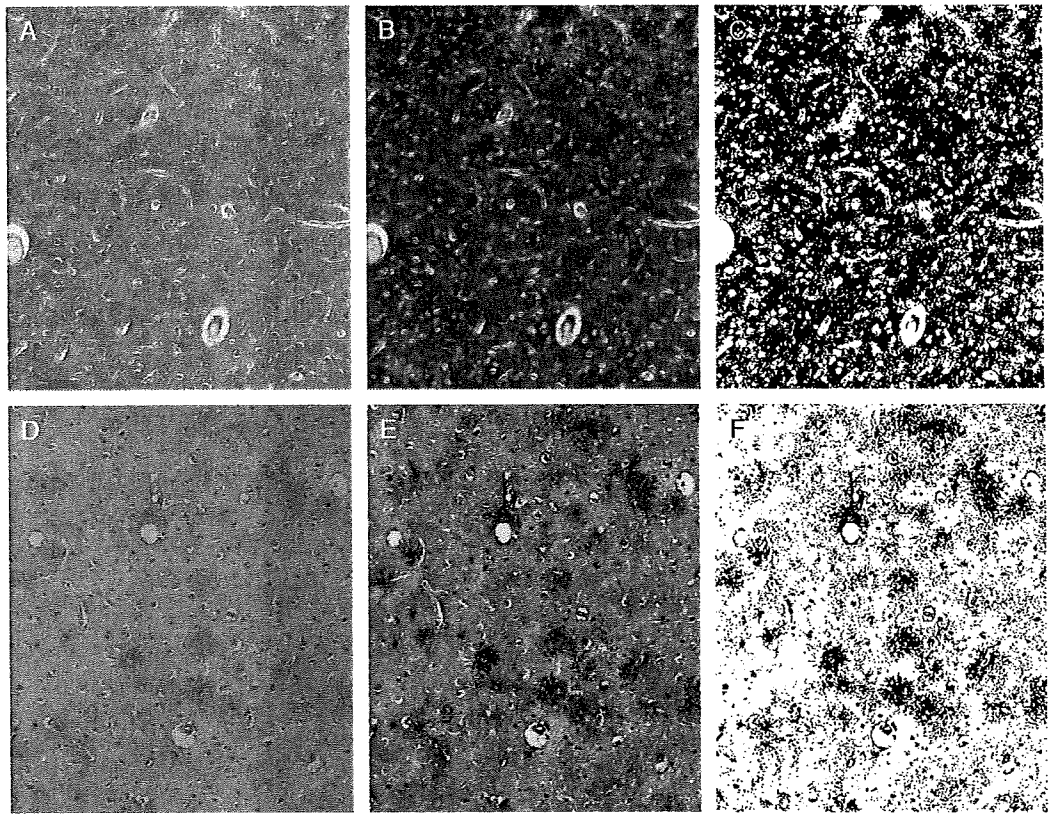

FIGURE 5. Representative images used for semiquantitative analysis of excitatory amino acid transporter 2 (EAAT-2) immunostaining in the frontal cortex. **(A–C)** Normal EAAT-2 staining pattern of more than 70% positive area in samples from an amyotrophic lateral sclerosis case (Patient 22) is shown in the EAAT-2 immunohistochemistry image (**[A]** original magnification: 100×), the blue-subtracted image (**[B]** original magnification: 100×), and the measured image by the National Institutes of Health (NIH) Image analysis program (**[C]** original magnification: 100×). **(D–F)** Decreased EAAT-2 immunostaining to approximately 10% positive area in sample from Patient 2 with human immunodeficiency virus 1 encephalitis is shown in the EAAT-2 immunohistochemistry image (**[D]** original magnification: 100×), the blue-subtracted image (**[E]** original magnification: 100×), and the measured image by the NIH Image analysis program (**[F]** original magnification: 100×).

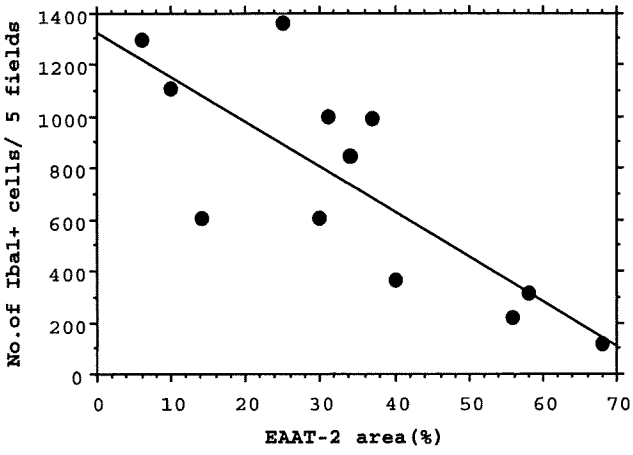

FIGURE 6. Relationship between the areas of excitatory amino acid transporter 2 (EAAT-2) expression and numbers of Iba1-positive microglia. There is a significant negative correlation between the areas of EAAT-2 expression and numbers of Iba1-positive microglia ($p < 0.01$, $R = -0.598$) among cases with decreased EAAT-2 expression.

there was strong immunopositivity for EAAT-2 in microglial cells, which was demonstrated in the double label immunohistochemical staining with anti-Iba1 and anti–EAAT-2 antibodies (Fig. 4D, arrows).

Correlation Between Activation of Microglia and Reduction of EAAT-2 Expression by Astrocytes in the Cerebral Cortex

In the 12 cases with decreased EAAT-2 expression, we assessed the correlation between the EAAT-2–positive areas and numbers of Iba1-positive microglia by Spearman rank correlation test and regression analysis (Fig. 5). A significant negative correlation was demonstrated between the areas of EAAT-2–positive areas and numbers of Iba1-positive microglia ($p < 0.01$, $R = -0.598$) among these cases (Fig. 6).

IL-1β and TNF Immunostaining in Inflammatory Lesions but Not in Diffusely Activated Microglia

Interleukin-1β was detected only in the cells of the inflammatory lesions in all 11 cases with HIVE (Figs. 7A, C); TNF was also detected in the inflammatory lesions of 7 cases with HIVE (Figs. 7B, D). In the cases without HIVE, IL-1β and TNF were detected in very few perivascular cells. Diffusely activated microglia in the frontal cortex did not show immunopositivity for these proinflammatory cytokines in any of the 12 cases with diffuse microglial activation (Figs. 7E–G). Semiquantitative assessments of the histopathologic findings in the frontal cortex are summarized in the Table.

DISCUSSION

We previously demonstrated that inflammation and cortical damage occur independently according to viral tropism in an SIV-infected macaque model of AIDS dementia (18); animals infected with T-cell tropic SIV developed advanced AIDS but no inflammatory changes in the brains (19). There was, however, primary injury to the astrocytes, including apoptosis and decreased EAAT-2 expression in the neuropil, diffuse activation of microglia, and limited neuronal damage. An apparent decrease in the EAAT-2 expression was observed in the animals with prolonged SIV infection. Apoptosis of the astrocytes and decreased EAAT-2 expression in the neuropil suggested that astrocytes are primarily involved in the cortical degeneration of AIDS encephalopathy. Some activated microglia also expressed EAAT-2 but not TNF and IL-1β, and SIV-infected cells were not detected in or around cortical lesions. These results suggested that astrocytic abnormalities and compensatory activation of microglia might provide a protective effect against neuronal degeneration in SIV-infected macaques without SIV encephalitis (19).

The results obtained in the present study are very similar to those of the SIV-infected macaque model. We observed various histopathologic changes in the frontal cortex of both HIVE and non-HIVE groups of HIV-1–infected patients, including diffuse microglial activation, apoptosis of astrocytes and neurons, and decreased EAAT-2 immunostaining. These cortical abnormalities were independent of the presence or absence of HIVE, as well as of its severity. It would be of great interest to identify a relationship between these pathological findings and the severity of the cognitive disorder in these cases, but this clinical information was not available. In this regard, an autopsy case of ADC has been reported in which prominent cortical atrophy and severe neuronal loss were observed, with minimal inflammatory changes in the white matter and basal ganglia (20). These observations suggest that HIVE and cortical degeneration may occur independently in HIV-1–infected individuals.

Petito and Roberts (21) reported evidence of apoptosis in neurons and astrocytes in HIV encephalitis and hypothesized that apoptosis of astrocytes may be a normal mechanism, whereby the brain removes excessive astrocytes that have proliferated after certain types of brain injury. In the present study, we examined proliferating cells in the frontal cortex by Ki-67 immunostaining and found that most of the positive cells were microglia rather than astrocytes by double label immunohistochemistry. This suggests that astrocytes may not proliferate in this condition, but astrocyte apoptosis supports the idea that they are primarily injured in HIV-infected individuals.

Another astrocytic change we observed was a remarkable decrease in the expression of EAAT-2 in the neuropil. Astrocytes are a major cellular component of the brain and have neuroprotective roles mediated by the expression of glutamate transporters (EAAT-1 and EAAT-2). Glutamate transporters maintain a low extracellular glutamate concentration in the brain and prevent excitotoxic neuronal cell death. Increase of extracellular glutamate is believed to be an important factor in the pathogenesis of many CNS disorders, including Huntington disease, Alzheimer disease, and multiple sclerosis (22–26). We believe, therefore, that in AIDS patients, injury to astrocytes results in a decrease of glutamate transporters in the cortex that enhances neuronal damage via excitotoxicity of glutamate.